Convexity and the Average Curvature of Plane Curves

Jeffrey C. Lagarias
AT&T Research
Murray Hill, NJ 07974
`jcl@research.att.com`

Thomas J. Richardson
Bell Laboratories
Murray Hill, NJ 07974
`tjr@research.bell-labs.com`

(June 18, 1996)

Abstract

The average curvature of a rectifiable closed curve in $\mathbb{R}^2$ is its total absolute curvature divided by its length. If a rectifiable closed curve in $\mathbb{R}^2$ is contained in the interior of a convex set D then its average curvature is at least as large as the average curvature of the simple closed curve ∂D which bounds the convex set.

Mathematics Subject Classification (1991): Primary 53A04, Secondary 52A10

Key Words: geometric inequalities, integral geometry, mean curvature, total curvature, convexity, plane curve.

Convexity and the Average Curvature of Plane Curves

Jeffrey C. Lagarias
AT&T Research
Murray Hill, NJ 07974

Thomas J. Richardson
Bell Laboratories
Murray Hill, NJ 07974

(June 18, 1996)

1 Introduction

A *curve* γ is a continuous map $\gamma : [a, b] \to \mathbb{R}^2$. It is *rectifiable* if its length $L(\gamma)$ is finite, and if it is C^2 then its *total absolute curvature* $K(\gamma)$ is

$$K(\gamma) := \int |\kappa(s)| ds \ , \tag{1.1}$$

where ds is arclength. More generally, we can define $K(\gamma)$ for rectifiable curves using polygonal approximations, in which case $K(\gamma) = +\infty$ is possible, see §2.

The *average curvature* $\mathcal{M}(\gamma)$ is defined by

$$\mathcal{M}(\gamma) := \frac{K(\gamma)}{L(\gamma)} \ . \tag{1.2}$$

(More precisely $\mathcal{M}(r)$ is the *average absolute curvature.*) The quantity $\mathcal{M}(\gamma)$ is well-defined up to strictly monotone reparametrization of the curve. It is invariant under Euclidean motions and satisfies

$$\mathcal{M}(r\gamma) = \frac{1}{r}\mathcal{M}(\gamma) \ , \text{ for } r > 0 \ . \tag{1.3}$$

The quantity $\mathcal{M}(\gamma)$ is a global invariant rather than a local invariant of γ, in the sense that locally a small arc of γ can have substantial length with little curvature (e.g. it can be a line segment), or alternatively, can have little length and substantial curvature.

The object of this paper is to prove inequalities for $\mathcal{M}(\gamma)$ related to convexity. Let D be a convex set with nonempty interior, with boundary ∂D. By an abuse of notation we also let

∂D denote the parametrized curve obtained using the parameter θ, $0 \le \theta \le 2\pi$, where $\partial D(\theta)$ denotes the point of intersection with the ray at angle θ from the centroid of D. Thus ∂D is a closed curve tracing out the boundary of D counterclockwise. Our main result is as follows.

Theorem 1.1 . *Let D be a compact convex set in $\mathbb{R}^2$ with nonempty interior. If γ is any closed rectifiable curve contained in D, then*

$$\mathcal{M}(\partial D) \le \mathcal{M}(\gamma) . \tag{1.4}$$

This result has long been known in the special case that D is a circular disk, where it follows from an inequality of Fáry [7] proved in 1950, which states that

$$L(\gamma) \le rK(\gamma) \tag{1.5}$$

where r is the radius of the smallest circular disk containing γ. More generally, Santaló [12, (3.26)] proves for closed piecewise C^2-curves γ the inequality

$$\frac{2}{\Delta_{\mathbf{m}}} \le \frac{K(\gamma)}{L(\gamma)} = \mathcal{M}(\gamma) , \tag{1.6}$$

in which $\Delta_{\mathbf{m}}$ is the maximal breadth of the convex hull D of γ. This inequality gives

$$\frac{2}{\Delta_{\mathbf{m}}} \le \mathcal{M}(\partial D) ,$$

which shows that the inequality (1.4) is a strengthening of (1.6).

We prove Theorem 1.1 for curves γ that are closed polygons $\mathcal{P}$, and then obtain the general case by a limiting argument. The proof for polygons is an argument by contradiction, which is given in §3 – §6. This proof does not settle the case of equality. We conjecture that equality holds if and only if γ is contained in ∂D, and is parameterization-equivalent to $k * \partial D$ for some integer $k \neq 0$. (Here $k * \partial D$ denotes the curve that traverses ∂D k times, where negative k connotes a reversal of the direction of traversal.)

Is convexity an essential hypothesis in Theorem 1.1? Consider for example the non-convex set S_a which consists of a unit square with a smaller square of side a removed from its upper right corner, which has $\mathcal{M}(\partial S_a) = \frac{3\pi}{4}$, cf. Figure 1.1(i). For $0 \le a < \frac{2}{3}$ the largest convex polygon P_a inscribed in S_a has $\mathcal{M}(\partial P_a) < \frac{3\pi}{4}$, but in the remaining range $\frac{2}{3} \le a < 1$ an

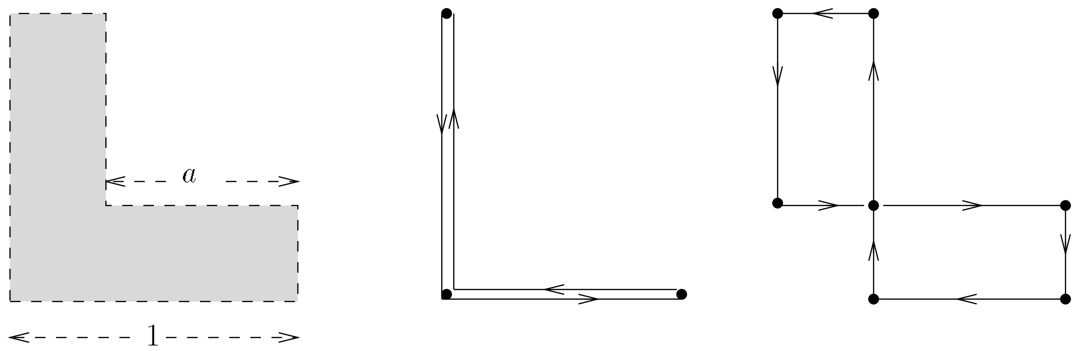

(i). Region S_a (ii). Curves with $\mathcal{M}(\gamma) = \frac{3\pi}{4}$

Figure 1.1: Nonconvex region $S_a (0 < a < 1)$

analogue of Theorem 1.1 may hold.

Conjecture. *For $\frac{2}{3} \leq a < 1$, and for any rectifiable closed curve γ contained in S_a,*

$$\mathcal{M}(\partial S_a) \leq \mathcal{M}(\gamma) . \tag{1.7}$$

This conjecture, if true, might conceivably be proved using arguments in the spirit of this paper. However there are definitely some extra complications to overcome. Figure 1.1 (ii) pictures some curves γ attaining equality $\mathcal{M}(\gamma) = \mathcal{M}(\partial S_a) = \frac{3\pi}{4}$. One of these curves contains a "jump," (using the terminology of §5) and this shows that the arguments of §5 cannot apply in this case. The existence of extremal curves with a "jump" also implies that the set of extremals would be strictly larger than the (conjectured) set of extremal curves for a convex set D.

There may well be valid n-dimensional generalizations of Theorem 1.1. For a convex body D in $\mathbb{R}^n$, the set ∂D is a convex closed hypersurface. There are subtle issues in formulating n-dimensional analogues of total curvature, so we restrict attention to the case of closed $(n-1)$-dimensional submanifolds γ that are C^2-immersed in $\mathbb{R}^n$. The *total mean curvature* of γ is

$$K_m(\gamma) := \int_\gamma |H| dV , \tag{1.8}$$

in which H is the mean curvature

$$H := \frac{1}{n+1}(k_1 + \cdots + k_{n-1}) ,$$

where $(k_1, \cdots, k_{n-1})$ are the curvatures at a point of γ. We define the *average mean curvature* by

$$\mathcal{M}_m(\gamma) := \frac{K_m(\gamma)}{\mathcal{H}^{n-1}(\gamma)} \ , \tag{1.9}$$

where $\mathcal{H}^{n-1}(\gamma)$ is the $(n-1)$-dimensional Hausdorff measure of γ, which satisfies $\mathcal{H}^{n-1}(\gamma) < \infty$ since γ is a C^2-immersion. The n-dimensional analogue of Fary's inequality, that

$$\mathcal{M}_m(\partial D) \leq \mathcal{M}_m(\gamma) \tag{1.10}$$

where $\gamma \subseteq D = B_n(r) = \{x \in \mathbb{R}^n : ||x|| \leq r\}$ is a result of Burago and Zalgaller [3, Theorem 28.2.5]. Their result applies to γ that are C^2-smooth immersions of manifolds with angles. We note that there is a polyhedral analogue of mean curvature, which traces back to work of Steiner [14] in 1840, and for which see Banchoff [1], [2], Chern [6]. For other curvature measures for polyhedra, see Flaherty [8] and Cheeger et al [4], [5].

It would seem natural to try to prove Theorem 1.1 using methods of integral geometry. There are elegant formulae for length (Crofton's formula) and also for total curvature, the latter appearing in Richardson [11]. At present we do not see how to obtain a proof of Theorem 1.1 using integral geometric methods. We have included integral-geometric proofs of some special cases (Lemmas 3.1 and 3.2) which are due to Joel L. Weiner, and replace our original elementary proofs.

Acknowledgments. We are indebted to Serge Tabachnikov for bringing this subject to our attention. He encountered the problem in the special case of the circular disk D as a Moscow Mathematical Olympiad problem, see Galperin and Topygo [9, Problem #33]. We are indebted to a Joel L. Weiner for several corrections.

2 Basic Facts and Preliminary Reductions

An (*oriented*) *curve* γ is a continuous mapping $\gamma : [a, b] \to \mathbb{R}^n$. It is *closed* if $\gamma(a) = \gamma(b)$. We define length $L(\gamma)$ for curves and total curvature $K(\gamma)$ for closed curves using polygonal approximations that respect the parametrization. A *polygonal curve* $\mathcal{P} = [v_0, v_1, \ldots, v_m]$ is specified by its ordered set of *vertices* $\{v_i : 0 \leq i \leq m\}$, and its image consists of the set of oriented line segments $[v_i, v_{i+1}]$. It is *closed* if $v_m = v_0$ and we then call $\mathcal{P}$ a *polygon* and denote it $\mathcal{P} = \langle v_0, v_1, \ldots, v_{m-1}\rangle$. We linearly parametrize $\mathcal{P}$ by arclength. We define the *length* $L(\mathcal{P})$

of a polygonal curve $\mathcal{P}$ by

$$L(\mathcal{P}) = \sum_{i=0}^{m-1} ||v_{i+1} - v_i|| \ ,$$

where $||\cdot||$ is Euclidean length. The *total absolute curvature* $K(\mathcal{P})$ of a polygon $\mathcal{P} = \langle v_0, v_1, \ldots, v_{n-1} \rangle$ is the sum of all the external angles between the oriented line segments $[v_i, v_{i+1}]$ and $[v_{i+1}, v_{i+2}]$ in the planes they determine, where by definition $[v_{m-1}, v_m] = [v_{-1}, v_0]$, i.e.

$$K(\mathcal{P}) = \sum_{i=0}^{m-1} (\pi - \text{ angle } (v_{i-1}, v_i, v_{i+1})) \ ,$$

where we adopt the convention that

$$0 \leq \text{ angle}(v_{i-1}, v_i, v_{i+1}) \leq \pi \ .$$

Thus external angles lie between 0 and π, see Figure 2.1. If v_{i-1}, v_i, v_{i+1} are collinear, then the external angle is 0 if v_i lies between v_{i-1} and v_{i+1}, and is π otherwise.

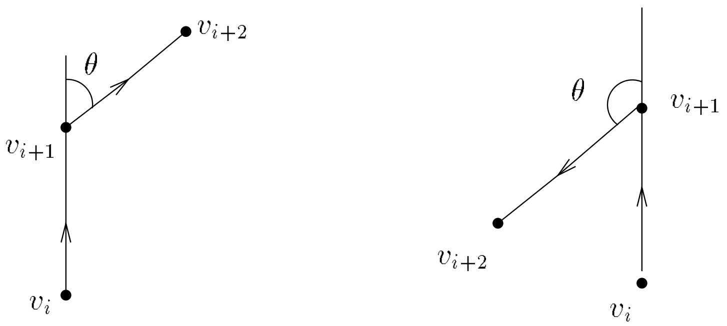

Figure 2.1: External angles

A polygonal curve is *inscribed* in a curve γ if $v_i = \gamma(t_i)$ where $a \leq t_1 < t_2 < \ldots < t_m \leq b$. The definition of length above extends to curves by

$$L(\gamma) := \sup\{L(\mathcal{P}) : \mathcal{P} \text{ is inscribed in } \gamma\} \tag{2.1}$$

For C^1-curves $L(\gamma)$ is equal to the usual definition of length. We say that γ is *rectifiable*[1] if $L(\gamma) < \infty$. For closed curves we define total absolute curvature by

$$K(\gamma) := \sup\{K(\mathcal{P}) : \mathcal{P} \text{ is a polygon inscribed in } \gamma\} \ . \tag{2.2}$$

[1]The *image* or *trace* of the curve γ is $\mathbf{c} = \gamma([a, b])$. A curve is called *rectifiable* if the one-dimensional Hausdorff measure $\mathcal{H}^1(\mathbf{c}) < \infty$. This coincides with the definition above, although $L(\gamma) > \mathcal{H}^1(\mathbf{c})$ may occur, when the parametrization traverses parts of $\mathbf{c}$ more than once.

This definition was suggested by Fox, see Milnor [10]. For C^2-curves it coincides with the definition (1.1).

If $\mathcal{P}_1$ and $\mathcal{P}_2$ are polygons inscribed in a closed curve γ, let $\mathcal{P}'$ denote their common refinement, i.e., $\mathcal{P}'$ is the inscribed polygon having vertices $v_i' = \gamma(t_i')$ where t_i' runs over all values of t_i for both $\mathcal{P}_1$ and $\mathcal{P}_2$. Then

$$\begin{aligned} L(\mathcal{P}') &\geq \max(L(\mathcal{P}_1), L(\mathcal{P}_2)) \ , \\ K(\mathcal{P}') &\geq \max(K(\mathcal{P}_1), K(\mathcal{P}_2)) \ . \end{aligned}$$

Consequently for any rectifiable curve γ, there exists a sequence $\{\mathcal{P}_i'\}$ of polygons inscribed in γ, such that $L(\mathcal{P}_i') \to L(\gamma)$ and $K(\mathcal{P}_i') \to K(\gamma)$ as $i \to \infty$. Thus there exist inscribed polygons P_i' in γ with

$$\mathcal{M}(\mathcal{P}_i') \to \mathcal{M}(\gamma) \quad \text{as} \quad i \to \infty \ . \tag{2.3}$$

The *parametrization equivalence class* of a curve γ consists of all strictly monotone reparametrizations of γ. If γ is a closed curve, we also allow a shift of base point (mod $(b-a)$) as an admissible reparametrization. Both definitions 2.1 and 2.2 are invariant under such reparametrizations.

From now on we consider only curves and sets in the plane $\mathbb{R}^2$. Given a set S let $\text{conv}(S)$ denote the convex hull of S. We first reduce Theorem 1.1 to the case that $D = \text{conv}(\gamma)$.

Lemma 2.1 *(i) If D is a bounded convex set in $\mathbb{R}^2$ then*

$$K(\partial D) = 2\pi \ .$$

(ii) If $D_1 \subseteq D_2$ are convex sets in $\mathbb{R}^2$ then

$$L(\partial D_1) \leq L(\partial D_2) \ ,$$

Proof. (i) This follows from Santaló [12], p. 113, observing that the curvature of ∂D has constant sign if D is convex.

(ii). This follows by integral geometry, using Crofton's formula for $L(\gamma)$. Alternatively, for a convex set in $\mathbb{R}^2$ we have

$$L(\partial D) = \frac{1}{2} V(D, B)$$

where $V(D, B)$ is the mixed volume of D and the unit ball B. Now (ii) follows from the monotonicity of mixed volumes in their arguments, cf. Schneider [13], (5.1.23). $\square$

Lemma 2.1 implies that if D_1 and D_2 are convex sets and $D_1 \subseteq D_2$, then

$$\mathcal{M}(\partial D_1) = \frac{2\pi}{L(\partial D_1)} \geq \frac{2\pi}{L(\partial D_2)} = \mathcal{M}(\partial D_2) \; . \tag{2.4}$$

Thus, to prove Theorem 1.1, it suffices to prove that

$$\mathcal{M}(\gamma) \geq \mathcal{M}(\partial \mathrm{conv}(\gamma)) \; . \tag{2.5}$$

We next reduce Theorem 1.1 to the special case of polygons.

Lemma 2.2 *If there exists a rectifiable curve γ contained in a convex set D such that $\mathcal{M}(\gamma) < \mathcal{M}(\partial D)$, then there exists a closed polygon $\mathcal{P}$ such that $\mathcal{M}(\mathcal{P}) < \mathcal{M}(\partial \mathrm{conv}(\mathcal{P}))$.*

Proof. Let γ and D satisfy the hypothesis of the lemma. As observed in (2.3), there exists a sequence of polygons $\mathcal{P}_i$ inscribed in γ such that $\mathcal{M}(\mathcal{P}_i) \to \mathcal{M}(\gamma)$. Choose $\mathcal{P} = \mathcal{P}_i$ with i taken so large that $\mathcal{M}(\mathcal{P}_i) < \mathcal{M}(\partial D)$. Since $\mathrm{conv}(\mathcal{P}) \subseteq D$, we have $\mathcal{M}(\partial D) \leq \mathcal{M}(\partial \mathrm{conv}(\mathcal{P}))$ by (2.4), hence $\mathcal{M}(\mathcal{P}) < \mathcal{M}(\mathrm{conv}(\mathcal{P}))$. $\square$

We will prove Theorem 1.1 in the polygonal case by contradiction, showing that any polygonal counterexample implies the existence of simpler polygonal counterexamples, until we in effect reduce to a critical case: a convex quadrilateral versus a nonconvex quadrilateral with the same vertices. In §3 we show there are no counterexamples in the critical case. Then, in §4–§6, we give the series of reductions culminating in Theorem 1.1.

Notational Conventions. In the remainder of the paper we use the following notation for polygons, rays and cones.

(1). $[v_0, \ldots, v_{n-1}]$ denotes a *polygonal arc* consisting of $n-1$ (oriented) line segments $[v_i, v_{i+1}]$, $0 \leq i \leq n-2$. (We sometimes group vertices using semicolons, e.g. $[v_0, \ldots, v_i; w_1, \ldots, w_j]$.)

(2). $\langle v_0, \ldots, v_{n-1} \rangle$ denotes a (closed) *polygon* $\mathcal{P}$. It consists of the n line segments $[v_i, v_{i+1}]$, $0 \leq i \leq n-1$, with $v_n = v_0$.

(3). $l[v_0, v_1]$ is the *line* through v_0 and v_1.
$l^+[v_0; v_1]$ is the (closed) *ray* $\{v_0 + \lambda v_1 : \lambda \geq 0\}$

(4.) $C^+[v_0; v_1, v_2]$ is the (closed) *cone* $\{v_0 + \lambda_1 v_1 + \lambda_2 v_2 : \lambda_1, \lambda_2 \geq 0\}$, which is pointed at v_0. $C^o[v_0; v_1, v_2]$ is the *open cone* $\{v_0 + \lambda_1 v_1 + \lambda_2 v_2 : \lambda_1 > 0, \lambda_2 > 0\}$, which is pointed at v_0.

(5). $\text{angle}(v_0, v_1, v_2)$ denotes the measure (in radians) of the angle determined by lines $l[v_0, v_1]$ and $l[v_1, v_2]$, with $0 \leq \text{angle}(v_0, v_1, v_2) \leq \pi$.

3 Quadrilaterals

The simplest polygonal case of the inequality of Theorem 1.1 is that between a convex quadrilateral $\mathcal{P}$ and nonconvex quadrilateral $\mathcal{P}'$ having the same convex hull. These are pictured in Figure 3.1, where for convenience we view the vertices of $\mathcal{P}$ oriented counterclockwise. We

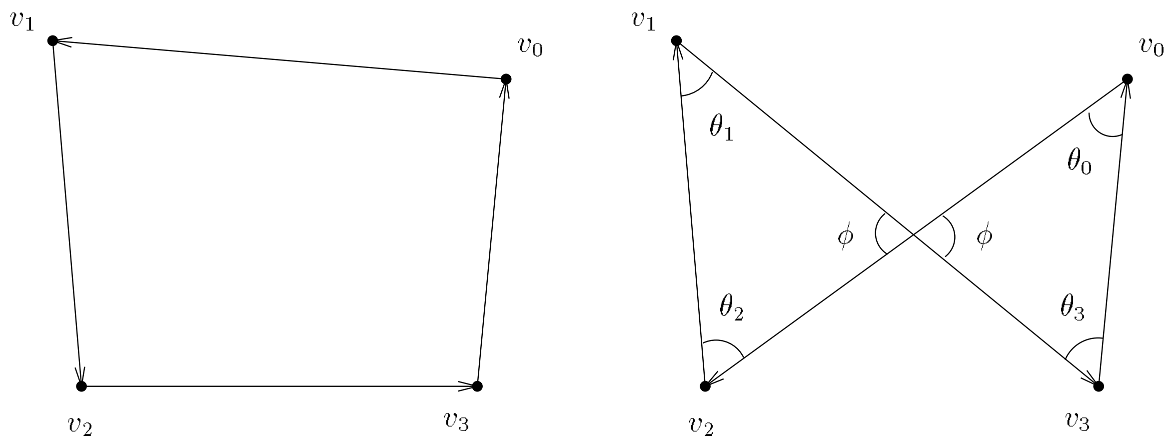

Figure 3.1: Convex and nonconvex quadrilaterals.

prove the following result.

Lemma 3.1 *Let $\mathcal{P} = \langle v_0, v_1, v_2, v_3\rangle$ be a convex quadrilateral and let $\mathcal{P}' = \langle v_0, v_2, v_1, v_3\rangle$ be one of the two nonconvex quadrilaterals (with two crossing edges) that have the same convex hull as $\mathcal{P}$. Then*

$$\mathcal{M}(\mathcal{P}') = \frac{K(\mathcal{P}')}{L(\mathcal{P}')} > \frac{K(\mathcal{P})}{L(\mathcal{P})} = \mathcal{M}(\mathcal{P}) \ . \tag{3.1}$$

Proof. We have $K(\mathcal{P}) = 2\pi$ while

$$K(\mathcal{P}') = \sum_{i=0}^{3}(\pi - \theta_i) = 4\pi - (2\pi - 2\phi) = 2(\pi + \phi) \tag{3.2}$$

where ϕ is the interior angle where the two edges of $\mathcal{P}'$ cross, see Figure 3.1. Thus the inequality (3.1) is equivalent to

$$\frac{2(\pi+\phi)}{\mathcal{L}(\mathcal{P}')} > \frac{2\pi}{\mathcal{L}(\mathcal{P})} \,. \tag{3.3}$$

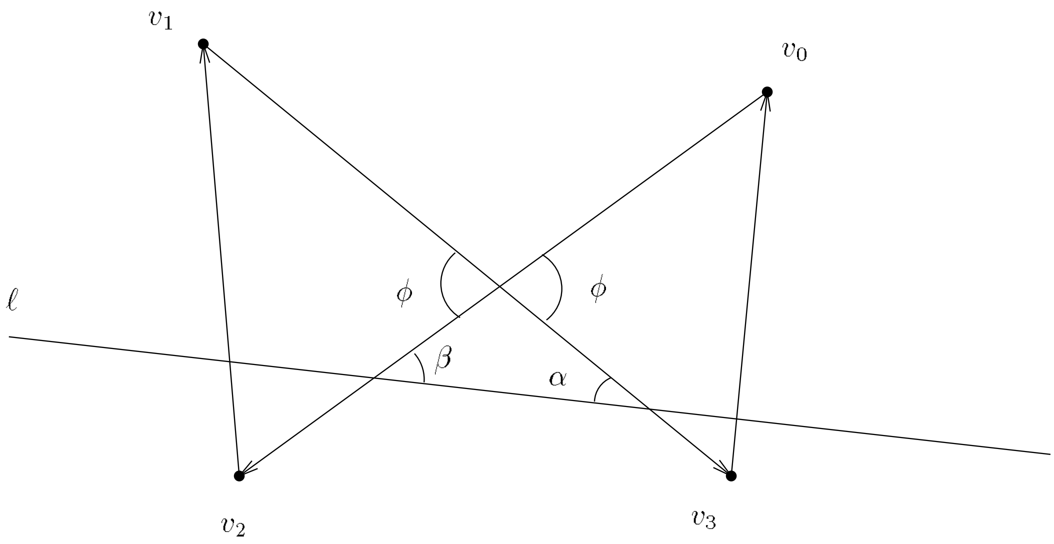

Figure 3.2: Line ℓ hitting nonconvex quadrilateral.

We prove the inequality by an integral-geometric argument. Let $\mathbb{H}$ denote the set of (unoriented) lines in $\mathbb{R}^2$ and ν denote the Haar measure for sets in $\mathbb{H}$ (invariant for Euclidean motions). If we parametrizes line ℓ in $\mathbb{R}^2$ by the data (x, θ) indicating that ℓ hits the x-axis at the point $(x, 0)$ with angle θ then the kinematic density $d\nu$ is given by

$$d\nu = |\sin(\theta)|\, dx\, d\theta \,,$$

(see Santalo [12, p. 29]). For a set $\mathcal{S} \subset \mathbb{R}^2$ and $k \geq 1$ let

$$[\mathcal{S}] := \{\ell \in \mathbb{H} : \ell \cap \mathcal{S} \neq \emptyset\}\,, \quad \text{and} \quad [\mathcal{S}]_k := \{\ell \in \mathbb{H} : |\ell \cap \mathcal{S}| = k\}\,.$$

For a polygon $\mathcal{P}$ with m sides Crofton's formula gives

$$\mathcal{L}(\mathcal{P}) = \frac{1}{2}\sum_{k=1}^{m} k\nu([\mathcal{P}]_k)\,,$$

cf. [12, p. 31] and Steinhaus [15]. Let $\nu_k = \nu([\mathcal{P}]_k)$ and $\nu'_k = \nu([\mathcal{P}']_k)$. Now, each line that hits $\mathcal{P}$ also hits $\mathcal{P}'$ and conversely, and, excluding a set of ν-measure zero, such a line hits $\mathcal{P}$ in two points and hits $\mathcal{P}'$ in either two or four points. Crofton's formula gives, $\mathcal{L}(\mathcal{P}) = \nu_2 = \nu'_2 + \nu'_4$ and $\mathcal{L}(\mathcal{P}') = \nu'_2 + 2\nu'_4$ hence the inequality (3.3) is equivalent to

$$\frac{\phi}{\pi} > \frac{\nu'_4}{\nu'_2 + \nu'_4}\,. \tag{3.4}$$

We now define some sets of lines associated to the nonconvex quadrilateral $\mathcal{P}'$. For $\ell \in \mathbb{H}$ let $\alpha \in [0, \pi)$ denote the angle through which the vector $v_1 - v_3$ must be rotated counter-clockwise to become tangent to ℓ and let $\beta \in [0, \pi)$ denote the angle through which the vector $v_0 - v_2$ must be rotated clockwise to become tangent to ℓ, see Figure 3.2. We set

$$\begin{aligned}
\mathcal{A} &:= \{\ell \in \mathbb{H} : \ell \text{ hits segment } [v_1, v_3]\} \\
\mathcal{A}' &:= \{\ell \in \mathbb{H} : \ell \in \mathcal{A} \text{ and } 0 \le \alpha \le \frac{\phi}{2}\} \\
\mathcal{B} &:= \{\ell \in \mathbb{H} : \ell \text{ hits segment } [v_0, v_2]\} \\
\mathcal{B}' &:= \{\ell \in \mathbb{H} : \ell \in \mathcal{B} \text{ and } 0 \le \beta \le \frac{\phi}{2}\}\,.
\end{aligned}$$

Now, $\ell \in [\mathcal{P}']_4$ implies that

$$\alpha + \beta = \phi\,,$$

see Figure 3.2. At least one of α or β is $\le \frac{\phi}{2}$, hence, $[\mathcal{P}']_4 \subset \mathcal{A}' \cup \mathcal{B}'$ which yields

$$\nu'_4 \le \nu(\mathcal{A}') + \nu(\mathcal{B}').$$

Next, $\mathcal{A} \subset [\mathcal{P}']$ and $\mathcal{B} \subset [\mathcal{P}']$, hence

$$\nu(\mathcal{A}) \le \nu'_2 + \nu'_4\,,$$

and

$$\nu(\mathcal{B}) \le \nu'_2 + \nu'_4\,.$$

Thus

$$\frac{\nu'_4}{\nu'_2 + \nu'_4} \le \frac{\nu(\mathcal{A}') + \nu(\mathcal{B}')}{\nu'_2 + \nu'_4} \le \frac{\nu(\mathcal{A}')}{\nu(\mathcal{A})} + \frac{\nu(\mathcal{B}')}{\nu(\mathcal{B})}.$$

Since $\nu(\cdot)$ is invariant under Euclidean motions, we may treat $\ell[v_1, v_3]$ as the x-axis centered at $v_1 = (0,0)$ with $v_3 = (L, 0)$ to obtain $\nu(\mathcal{A}) = 2\,L = 2\,\|v_1 - v_3\|$ while

$$\nu(\mathcal{A}') = \int_0^L \int_0^{\frac{\phi}{2}} \sin(\alpha)\, d\alpha\, dx\,,$$

hence

$$\frac{\nu(\mathcal{A}')}{\nu(\mathcal{A})} = \frac{1}{2}(1-\cos(\frac{\phi}{2}))\,.$$

A similar bound holds for $\frac{\nu(\mathcal{B}')}{\nu(\mathcal{B})}$, hence we obtain

$$\frac{\nu_4'}{\nu_2'+\nu_4'} \leq 1-\cos(\frac{\phi}{2})\,.$$

We conclude that (3.4) is implied by

$$\frac{\phi}{\pi} > 1-\cos(\frac{\phi}{2}),\;\; 0<\phi<\pi\,.$$

This follows easily by the strict convexity of $1-\cos(\frac{\phi}{2})$ for $0 \leq \phi \leq \pi$. □

For later application we generalize Lemma 3.1 to cover the case of a quadrilateral contained inside a larger convex polygon, see Figure 3.3.

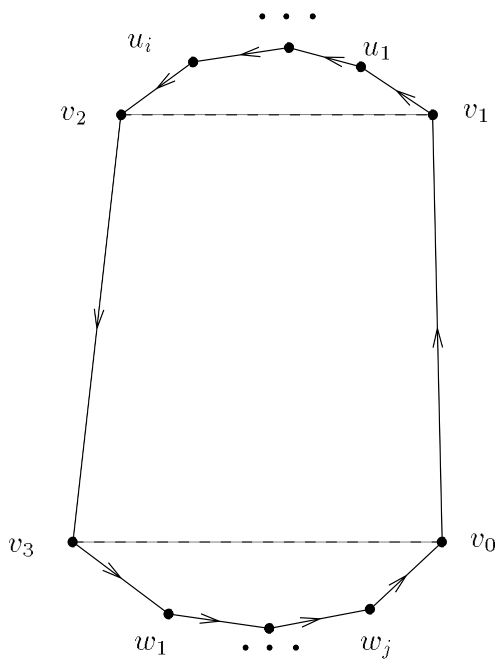

(i). Convex P

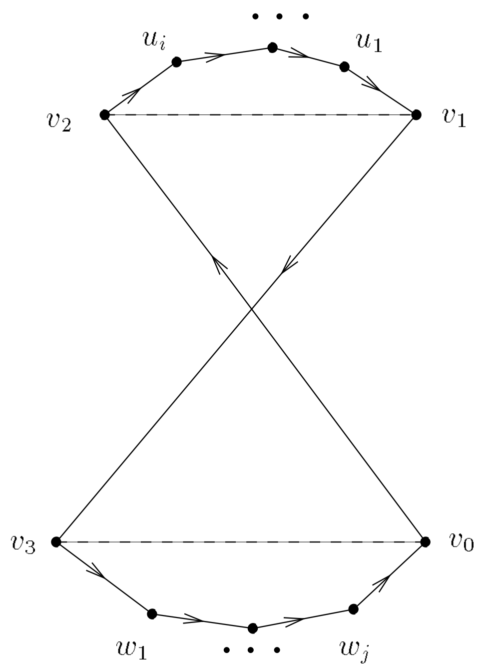

(ii). Nonconvex P'

Figure 3.3: Generalized quadrilaterals P and P'

Lemma 3.2 *Let* $\mathcal{P} = \langle v_0, v_1; u_1, \ldots, u_i; v_2, v_3; w_1, \ldots, w_j \rangle$ *be a convex polygon having no three collinear vertices, and set*

$$\mathcal{P}' := \langle v_0, v_2; u_i, u_{i-1}, \ldots, u_1; v_1, v_3; w_1, \ldots, w_j \rangle$$

Then

$$\mathcal{M}(\mathcal{P}') > \mathcal{M}(\mathcal{P}) \ . \tag{3.5}$$

Proof. The situation is pictured in Figure 3.3, where we assume a counterclockwise orientation of $\mathcal{P}$ for definiteness. The proof given for Lemma 3.1 goes through in the generalized case. Note that $K(\mathcal{P}') = 2(\pi + \phi)$ is still valid. □

4 Reduction Theorem: Removing Interior Vertices

We will prove Theorem 1.1 by contradiction. By Lemma 2.2 we may assume the existence of a polygonal counterexample. The basic strategy of the proof is to deduce the existence of simpler and simpler polygonal counterexamples, until a contradiction is obtained. Henceforth a *CX-polygon* $\mathcal{P}$ is a polygonal counterexample to Theorem 1.1, i.e., one with

$$\mathcal{M}(\mathcal{P}) < \mathcal{M}(\partial \mathrm{conv}(\mathcal{P})) \ . \tag{4.1}$$

Our object in this section is to prove:

Theorem 4.1 *If a CX-polygon exists, then there exists a CX-polygon* $\mathcal{P}'$ *such that all vertices of* $\mathcal{P}'$ *lie on* $\partial \mathrm{conv}(\mathcal{P}')$.

We call such a polygon $\mathcal{P}'$ a *boundary CX-polygon.* We begin with two preliminary lemmas.

Lemma 4.2 *Let* $\mathcal{P} = \langle v_0, v_1, \ldots, v_{n-1} \rangle$ *be a convex polygon. If* θ_0 *and* θ_1 *denote the interior angles at* v_0 *and* v_1*, respectively, then*

$$\frac{2(\theta_0 + \theta_1)}{L(\mathcal{P}) - 2||v_1 - v_0||} \geq \frac{2\pi}{L(\mathcal{P})} \ . \tag{4.2}$$

Proof. If $\theta_0 + \theta_1 \geq \pi$ the inequality is immediate. So suppose $\theta_0 + \theta_1 < \pi$, in which case the inequality to prove becomes

$$4\pi ||v_1 - v_0|| \geq 2(\pi - \theta_0 - \theta_1) L(\mathcal{P}) \ . \tag{4.3}$$

Since $\theta_0 + \theta_1 < \pi$ there is a triangle T having side $[v_0, v_1]$ and angles θ_0 and θ_1 at vertices v_0 and v_1, respectively. The convexity of $\mathcal{P}$ implies that the curve $\mathcal{P}$ lies inside or on T, i.e., $\text{conv}(\mathcal{P}) \subseteq \text{conv}(T)$, see Figure 4.1. Thus $L(T) \geq L(\mathcal{P})$, by Lemma 2.1. Therefore it suffices to prove

$$\frac{\|v_1 - v_0\|}{L(T)} \geq \frac{\theta}{2\pi} \tag{4.4}$$

where $\theta = \pi - \theta_0 - \theta_1$ is the apex angle of triangle T, see Figure 4.1.

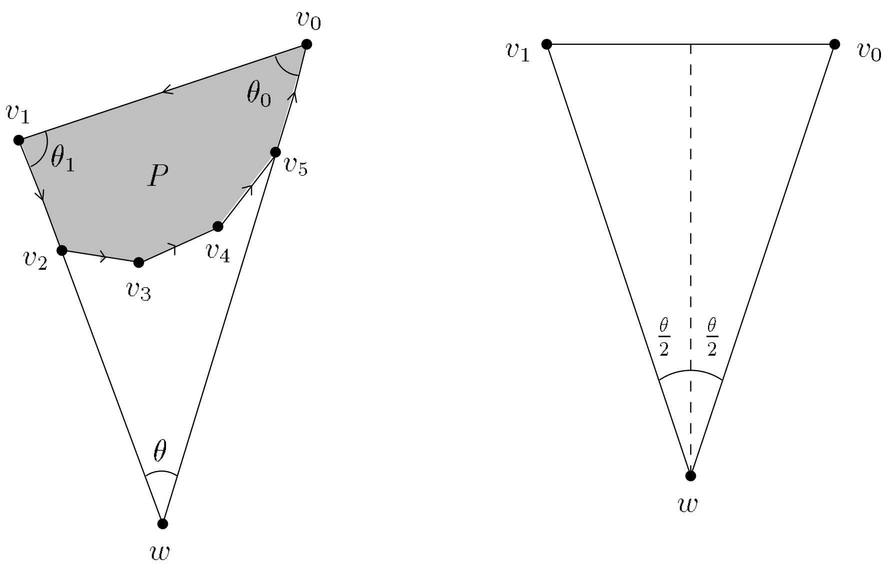

(i) General case (ii)

Figure 4.1: Circumscribing triangle T for P

Holding θ fixed, the largest value of $L(T)/||v_0 - v_1||$ is attained for an isosceles triangle, as can be seen by making a small variation in θ_0. For this triangle

$$L(T) = \|v_0 - v_1\| \left(\frac{1}{\sin \frac{\theta}{2}} + 1 \right) ,$$

cf. Figure 4.1. To prove (4.4) it thus suffices to show that

$$\frac{\theta}{2\pi} \leq \left(\frac{1}{\sin \frac{\theta}{2}} + 1 \right)^{-1} . \tag{4.5}$$

Now, $f(\theta) := \left(\frac{1}{\sin \frac{\theta}{2}} + 1 \right)^{-1}$ is strictly concave on $[0, \pi]$ since $\ddot{f}(\theta) = -\frac{1}{4} \frac{1+\sin \frac{\theta}{2} + \cos^2 \frac{\theta}{2}}{(1+\sin \frac{\theta}{2})^3}$, and (4.5) follows easily. $\square$

The key inequality (4.4) in the proof of Lemma 4.2 also has an integral-geometric proof which relates it to Lemma 3.1, as was observed by the referee.

Let I denote the line segment $[v_0, v_1]$ in triangle $\mathcal{T}$. Crofton's formula gives $\nu([I]) = 2\|v_0 - v_1\|$, and also gives $\nu([\mathcal{T}]) = L(\mathcal{T})$, because ν-almost every line that hits $\mathcal{T}$ hits it twice. Thus (4.4) is equivalent to

$$p = \frac{\nu([I])}{\nu([\mathcal{T}])} \geq \frac{\theta}{\pi}. \tag{4.6}$$

Consider now a configuration Q consisting of the triangle $\mathcal{T}$ together with a copy $\mathcal{T}'$ of $\mathcal{T}$ obtained by rotating $\mathcal{T}$ by angle π around its vertex w, with vertices v_0', v_1', w, see Figure 4.2.

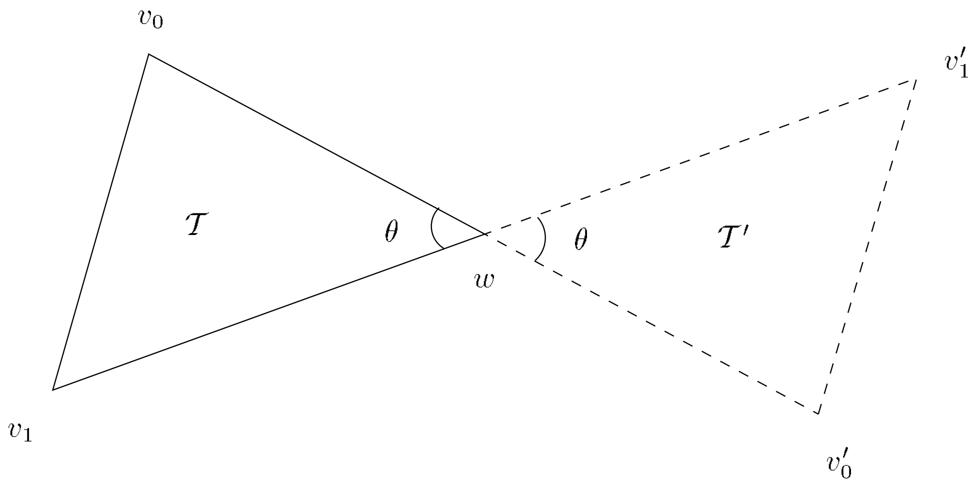

Figure 4.2: Reflected Triangle

Now, p is the probability that a line that hits $\mathcal{T}$ also hits I, so its complement $q = 1 - p$ is the probability that a line that hits $\mathcal{T}$ hits both $[v_0, w]$ and $[v_1, w]$. The nonconvex quadrilateral $Q' = [v_1', v_1, v_0', v_0]$ (not the quadrilateral pictured in Figure 4.2) has interior angle $\phi = \pi - \theta$. The lines that hit Q' four times are exactly the lines that hit $\mathcal{T}$ in both $[v_0, w]$ and $[v_1, w]$ or that hit $\mathcal{T}'$ in both $[v_0', w]$ and $[v_1', w]$, while those that hit Q' twice are exactly those lines that hit $[v_0, v_1]$ or $[v_0', v_1']$, hence $\nu([Q']_4) = 2\,\nu(\mathcal{W})$, where

$$\mathcal{W} := \{\ell \in \mathbb{H} : \ell \cap [v_0, w] \neq \emptyset \text{ and } \ell \cap [v_1, w] \neq \emptyset\}.$$

Since every line that hits Q' hits $\mathcal{T}$ or $\mathcal{T}'$ or both,

$$\nu([Q']) \leq \nu([\mathcal{T}]) + \nu([\mathcal{T}']) = 2\,\nu([\mathcal{T}])$$

Thus, using (3.4)

$$q = \frac{\nu(\mathcal{W})}{\nu([\mathcal{T}])} \leq \frac{\nu([Q']_4}{\nu([Q'])} \leq \frac{\pi - \theta}{\pi},$$

which proves (4.6).

Lemma 4.3 *Let $\mathcal{P} = \langle v_0, v_1, \ldots, v_{n-1} \rangle$ be a CX-polygon. Suppose that, for some i and j with $2 \leq j - i \leq n-2$, the polygon $\mathcal{Q} = \langle v_i, v_{i+1}, \ldots, v_j \rangle$ is convex, the vertex v_{i-1} lies in the closed cone*

$C^+[v_i; v_i - v_j, v_{i+1} - v_i]$ and that the vertex v_{j+1} lies in the closed cone $C^+[v_j; v_j - v_i, v_{j-1} - v_j]$. Then $\mathcal{P}' = \langle v_0, \ldots, v_i; v_j, v_{j+1}, \ldots, v_{n-1} \rangle$ has $\mathcal{M}(\mathcal{P}') < \mathcal{M}(\mathcal{P})$, and $\mathcal{P}'$ is a CX-polygon.

Remark. Note that this lemma applies in "degenerate" cases where v_{j+1} lies on the line $\ell[v_{j-1}, v_j]$ and where v_{i-1} lies on the line $\ell[v_i, v_{i+1}]$.

Proof. The hypotheses are pictured in Figure 4.3.

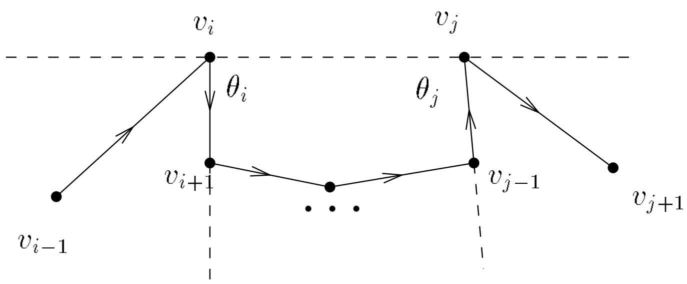

Figure 4.3: Configuration in Lemma 4.3.

Note that $v_i \neq v_j$, and v_{i-1} may lie on $l[v_i, v_j]$ to the left of v_i, and v_{j+1} may lie on the line to the right of v_j (in Figure 4.3).

Let θ_i = angle (v_{i+1}, v_i, v_j) and θ_j = angle (v_i, v_j, v_{j-1}). Certainly

$$L(\mathcal{P}') = L(\mathcal{P}) - (L(\mathcal{Q}) - 2||v_i - v_j||) .$$

and the convexity of $\mathcal{Q}$ yields

$$K(\mathcal{P}') = K(\mathcal{P}) - 2(\theta_i + \theta_j) .$$

Now the CX-polygon property of $\mathcal{P}$ states that

$$\mathcal{M}(\mathcal{P}) < \frac{K(\partial \mathrm{conv}(\mathcal{P}))}{L(\partial \mathrm{conv}(\mathcal{P}))} = \frac{2\pi}{L(\partial \mathrm{conv}(\mathcal{P}))} .$$

Since $\mathrm{conv}(\mathcal{Q}) \subseteq \mathrm{conv}(\mathcal{P})$, we have

$$\mathcal{M}(\mathcal{P}) < \frac{2\pi}{L(\partial \mathrm{conv}(\mathcal{P}))} \leq \frac{2\pi}{L(\mathcal{Q})} \leq \frac{2(\theta_i + \theta_j)}{L(\mathcal{Q}) - 2||v_i - v_j||} ,$$

where Lemma 2.1 and Lemma 4.2 were used. However, this yields

$$\mathcal{M}(\mathcal{P}') = \frac{K(\mathcal{P}) - 2(\theta_i + \theta_j)}{L(\mathcal{P}) - (L(\mathcal{Q}) - 2||v_i - v_j||)} < \mathcal{M}(\mathcal{P}) , \tag{4.7}$$

Since $\mathrm{conv}(\mathcal{P}') \subseteq \mathrm{conv}(\mathcal{P})$, (2.4) gives $\mathcal{M}(\partial \mathrm{conv}(\mathcal{P}')) \geq \mathcal{M}(\partial \mathrm{conv}(\mathcal{P}))$, hence $\mathcal{P}'$ is a CX-polygon. □

For later use we state a limiting case of Lemma 4.3.

Lemma 4.4 *Let $\mathcal{P} = \langle v_0, v_1, \ldots, v_{n-1} \rangle$ be a CX-polygon. Suppose that $v_j = v_i$ for some i and j with $2 \leq j - i \leq n-2$, the polygon $\mathcal{Q} = [v_i, v_{i+1}, \ldots, v_j]$ is convex, and there is a supporting line $\ell[v_i, w]$ to $\mathcal{Q}$ at v_i, such that w lies on the same side of $\ell[v_i, v_{i+1}]$ as v_{j-1}, the vertex v_{i-1} lies in the closed cone $C^+[v_i; v_i - w, v_{i+1} - v_i]$, and the vertex v_{j+1} lies in the closed cone $C^+[v_j; w - v_j, v_{j-1} - v_j]$. Then $\mathcal{P}' = \langle v_0, v_1, \ldots, v_i, v_{j+1}, \ldots, v_{n-1} \rangle$ has $\mathcal{M}(\mathcal{P}') < \mathcal{M}(\mathcal{P})$, and $\mathcal{P}'$ is a CX-polygon.*

Proof. The situation is pictured in Figure 4.4.

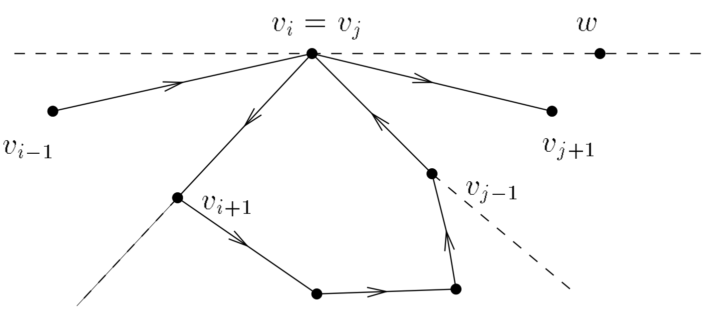

Figure 4.4: Configuration in Lemma 4.4.

This situation arises from Lemma 4.3 in the limit as $v_j \to v_i$ along the support ray $\ell^+[v_i; w - v_i]$. Note that both v_{i-1} and v_{j+1} are permitted to lie on the support line $\ell[v_i, w]$.

By considering internal angles at v_i, we find that

$$K(\mathcal{P}) - K(\mathcal{P}') \geq 2\pi ,$$

while

$$L(\mathcal{P}) - L(\mathcal{P}') = L(\mathcal{Q}) = L(\partial\text{conv}(\mathcal{Q})) \leq L(\partial\text{conv}(\mathcal{P})) \; .$$

Then, since $\mathcal{P}$ is a CX-polygon,

$$\mathcal{M}(\mathcal{P}') = \frac{K(\mathcal{P}')}{L(\mathcal{P}')} \leq \frac{K(\mathcal{P}) - 2\pi}{L(\mathcal{P}) - L(\partial\text{conv}(\mathcal{P}))} < \mathcal{M}(\mathcal{P}) < \mathcal{M}(\partial\text{conv}(\mathcal{P})) \leq \mathcal{M}(\partial\text{conv}(\mathcal{P}')) \; ,$$

so $\mathcal{P}'$ is a CX polygon. □

Proof of Theorem 4.1. It suffices to show that if there exists a CX-polygon $\mathcal{P}$ which has $m \geq 1$ interior vertices, then there exists a CX-polygon having strictly fewer than m interior vertices. The theorem then follows by downward induction on m.

We give three reductions below. Each reduction produces a new CX-polygon $\mathcal{P}'$, in which $\mathcal{P}'$ has fewer interior vertices than $\mathcal{P}$, and which every vertex of $\mathcal{P}'$ is a vertex of $\mathcal{P}$. Later we prove that one of these reductions applies to any CX-polygon $\mathcal{P}$.

Reduction I1. $\mathcal{P}$ contains three collinear vertices v_{i-1}, v_i, v_{i+1} such that v_i is an interior vertex.

This situation is pictured in Figure 4.5.

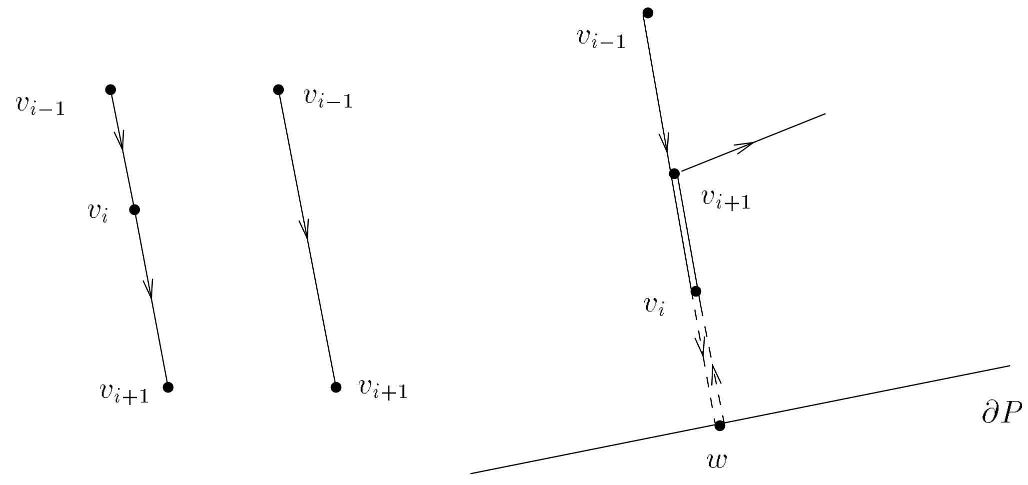

(i). Case (a)
(ii). Case (b)

Figure 4.5: Reduction I1

Case (a). If v_i separates v_{i-1} from v_{i+1} then we may just delete v_i.

Case (b). If v_{i-1} and v_{i+1} lie on the same side of $\ell[v_{i-1}, v_i]$ from v_i, then the polygon $\mathcal{P}$ has exterior angle π at v_i. Now prolong the ray $\ell^+[v_{i-1}; v_i - v_{i-1}]$ until it hits a boundary point w of conv($\mathcal{P}$). Replacing v_i with w, we obtain

$$\mathcal{P}' = \langle v_0, v_1, \ldots, v_{i-1}, w, v_{i+1}, \ldots, v_{m-1} \rangle$$

and $K(\mathcal{P}') = K(\mathcal{P})$ since there is still an exterior angle π at w, while $L(\mathcal{P}') > L(\mathcal{P})$. Thus $\mathcal{M}(\mathcal{P}') < \mathcal{M}(\mathcal{P})$ so $\mathcal{P}'$ is a CX-polygon.

Reduction I2. $\mathcal{P}$ contains an arc $[v_{i-1}, v_i, v_{i+1}, v_{i+2}]$ such that v_{i-1} and v_{i+2} are on the same side of the line $\ell[v_i, v_{i+1}]$, i.e., are in the same closed half-space. Furthermore at least one of v_i or v_{i+1} is an interior point of conv($\mathcal{P}$) *and at least one of v_{i-1} and v_{i+2} is not on the line $\ell[v_i, v_{i+1}]$.*

This situation is pictured in Figure 4.6. For definiteness let v_i be an interior point. If

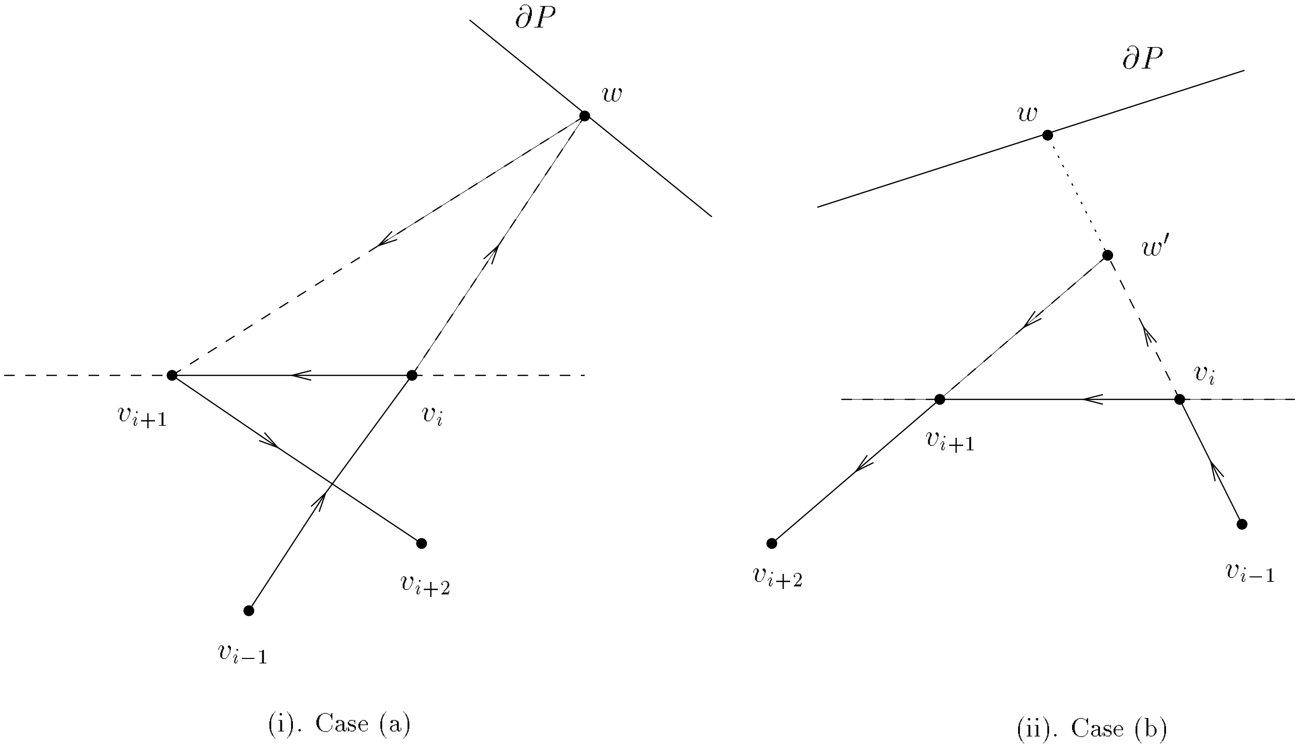

Figure 4.6: Reduction I2

v_{i-1}, v_i, v_{i+1} are collinear then reduction I1 applies. Therefore we may assume that v_{i+1} is in an open half-space determined by $\ell[v_{i-1}, v_i]$; we allow the possibility that v_i, v_{i+1}, v_{i+2} are collinear. Now extend the ray $\ell^+[v_{i-1}; v_i - v_{i-1}]$ until it hits the boundary $\partial\text{conv}(\mathcal{P})$ at a point w. There are two cases.

Case (a). The ray $\ell^+[v_{i+1}; v_{i+1} - v_{i+2}]$ does not intersect the open line segment (v_i, w). See Figure 4.6(i). Set

$$\mathcal{P}' = \langle v_0, \ldots, v_{i-1}, w, v_{i+1}, \ldots, v_{n-1} \rangle \ .$$

Then $K(\mathcal{P}') = K(\mathcal{P})$ and $L(\mathcal{P}') > L(\mathcal{P})$, while $\text{conv}(\mathcal{P}') = \text{conv}(\mathcal{P})$, so P' is a CX-polygon with the same number of vertices as $\mathcal{P}$ and one fewer interior vertex.

Case (b). The ray $\ell^+[v_{i+1};\ v_{i+1} - v_{i+2}]$ intersects the open line segment (v_i, w) at a point w', see Figure 4.6(ii). Now w' is an interior point of $\text{conv}(\mathcal{P})$, hence v_{i+1} must be an interior point of $\text{conv}(\mathcal{P})$. Set

$$\mathcal{P}' = \langle v_0, \ldots, v_{i-1}, w', v_{i+2}, \ldots, v_{n-1} \rangle \ .$$

Then $K(\mathcal{P}') = K(\mathcal{P})$ and $L(\mathcal{P}') > L(\mathcal{P})$, while $\text{conv}(\mathcal{P}') = \text{conv}(\mathcal{P})$, so P' is a CX-polygon with one fewer vertex and one fewer interior vertex than $\mathcal{P}$.

Reduction I3. $\mathcal{P}$ contains an arc $[v_{i-1}, v_i, v_{i+1}, v_{i+2}, v_{i+3}]$ such that $\langle v_i, v_{i+1}, v_{i+2}\rangle$ is a triangle and v_{i+1} is an interior point of $\text{conv}(\mathcal{P})$. *Furthermore v_{i-1} lies in the closed cone $C^+[v_i; v_i - v_{i+2}, v_{i+1} - v_i]$ and v_{i+3} lies in the closed cone $C^+[v_{i+2}; v_{i+2} - v_i, v_{i+1} - v_{i+2}]$.*

In this case Lemma 4.3 applies with $Q = \langle v_i, v_{i+1}, v_{i+2}\rangle$, to conclude that

$$\mathcal{P}' = \langle v_0, v_1, \ldots, v_{i-1}, v_i, v_{i+2}, \ldots, v_{n-1}\rangle$$

is a CX-polygon. Also $\text{conv}(\mathcal{P}') = \text{conv}(\mathcal{P})$ since v_i is an interior point of $\text{conv}(\mathcal{P})$, and $\mathcal{P}'$ has one fewer vertex and one fewer interior vertex than $\mathcal{P}$.

Induction Step. We assume that $\mathcal{P}$ has at least one interior vertex, and without loss of generality suppose that $v_1 \in \partial\text{conv}(\mathcal{P})$ and that v_2 is an interior vertex. We now claim that at least one of reductions I1, I2 or I3 applies to $\mathcal{P}$. To show this, we consider cases.

(1). If v_1, v_2, v_3 are collinear then reduction I1 apples to remove v_2 as an interior vertex. Thus we may suppose that v_3 does not lie on the line $\ell[v_1, v_2]$.

(2). If v_0 and v_3 lie in the same closed half space determined by $\ell[v_1, v_2]$, then reduction I2 applies, since v_3 lies in an open half-space determined by $\ell[v_1, v_2]$. Thus we may suppose that v_0 and v_3 are in opposite open half-spaces determined by $\ell[v_1, v_2]$, as pictured in Figure 4.7.

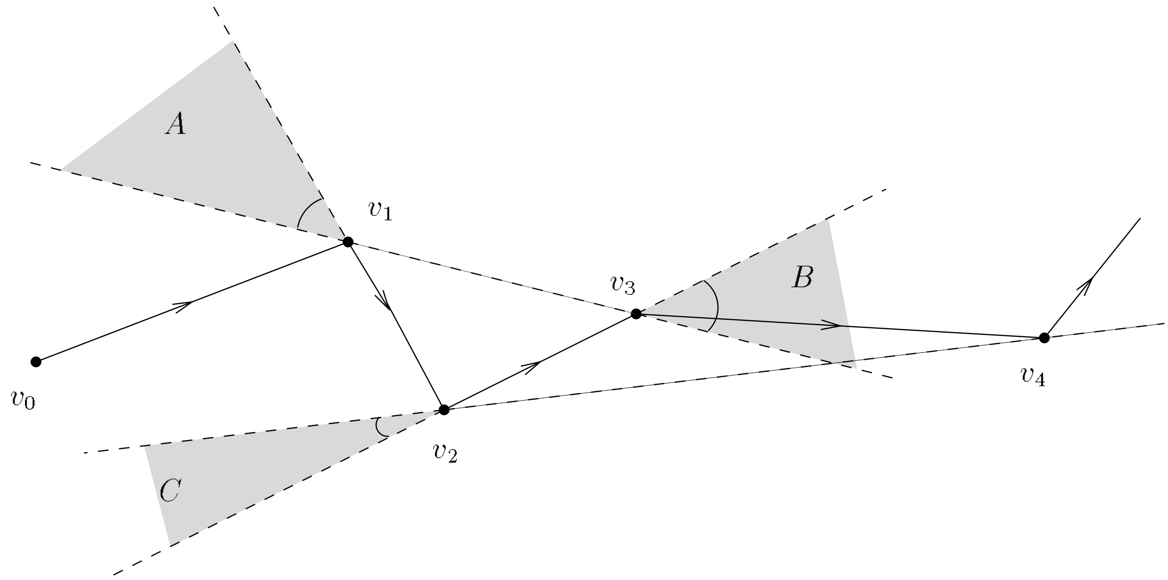

Figure 4.7: Non-reducible configuration

(3). If v_2, v_3, v_4 are collinear and v_3 is an interior point, reduction I1 applies.

(4). Suppose v_2, v_3, v_4 are collinear and that $v_3 \in \partial\text{conv}(\mathcal{P})$. Then v_4 is on the same side of the line $\ell[v_1, v_3]$ as v_2. If v_2 did not lie on the same side of the line $\ell[v_1, v_3]$ as v_0, then (by (2)) v_0 must lie in the open cone $C^o[v_1; v_1 - v_2, v_1 - v_3]$, which is marked A in Figure 4.6. If so, then v_1 lies strictly inside the triangle $\langle v_0, v_2, v_3\rangle$, contradicting $v_1 \in \partial\text{conv}(P)$. Thus v_2 must lie on the same side of the line $\ell[v_1, v_3]$ as v_0, hence v_0 and v_4 are on the same side of the line $l[v_1, v_3]$, so reduction I3 applies to $[v_0, v_1, v_2, v_3, v_4]$.

(5). There remains the case that v_2, v_3, v_4 are not collinear. If v_4 is in the same open half-space as v_1, with respect to the line $\ell[v_2, v_3]$, then reduction I2 applies. Thus we may suppose that v_4 is in the open half space on the other side of $\ell[v_2, v_3]$.

(6). If v_4 is also in the closed half-space determined by $\ell[v_1, v_3]$ that contains v_2, hence v_0, then reduction I3 applies to $[v_0, v_1, v_2, v_3, v_4]$.

(7). There remains the case that v_4 lies in the open cone $C^o[v_3; v_3 - v_2, v_3 - v_1]$, which is marked B in Figure 4.7. In this case v_3 is in the interior of the triangle $\langle v_1, v_2, v_4\rangle$, hence it is an interior point of $\mathcal{P}$.

(8). We can now repeat the argument of steps (1)–(7), starting with the configuration v_1, v_2, v_3, v_4 in which v_3 is strictly inside the triangle $\langle v_1, v_2, v_4\rangle$. Here we note that (1)–(7) did not use the full strength of the property that v_1 was a boundary point, but only used in step (4) the weaker property that $v_0 \notin C^o[v_1; v_1 - v_2, v_1 - v_3]$. The equivalent property that $v_1 \notin C^o[v_2; v_2 - v_3, v_2 - v_4]$ follows from v_3 being in the interior of the triangle $\langle v_1, v_2, v_4\rangle$. (Here $C^o[v_2; v_2 - v_3, v_2 - v_4]$ is the open cone labeled C in Figure 4.7.) We conclude that at least one of the reductions I1–I3 applies, unless v_4 is strictly inside the triangle $\langle v_2, v_3, v_5\rangle$. Thus v_4 is an interior vertex.

(9). Continuing similarly, we get a reduction unless v_{i+2} is contained in the interior of triangle $\langle v_i, v_{i+1}, v_{i+3}\rangle$, for all $i \geq 1$. Thus all vertices v_{i+2} are interior vertices, which contradicts the fact that $\mathcal{P}$ has at least one vertex on $\partial\mathrm{conv}(\mathcal{P})$. This contradiction shows that one of the reductions I1–I3 must apply. $\Box$

5 Reduction Theorem: Removing Jumps

We now have reduced to the case of a CX-polygon $\mathcal{P}$ having all vertices v_i on its boundary $\partial\mathrm{conv}(\mathcal{P})$, i.e., $\mathcal{P}$ is a *boundary CX-polygon.* Given a line segment $[v_i, v_{i+1}]$ in $\mathcal{P}$, we call it a *jump* if it is not entirely contained in the boundary $\partial\mathrm{conv}(\mathcal{P})$. In this section we prove the following reduction theorem.

Theorem 5.1 *If there exists a boundary CX-polygon, then there exists a boundary CX-polygon which has no jumps.*

As a preliminary simplification, we show that we may suppose that the boundary CX-polygon has no three collinear vertices. To achieve this, we first add extra vertices so that no edge contains any vertex v_j of the polygon in its interior. That is, if the interior of an edge $[v_i, v_{i+1}]$ passes through a vertex v_j, then this edge $[v_i, v_{i+1}]$ is split in two by adding a new vertex

$v_i' = v_j$. After this is done, all midpoint vertices in a set of collinear vertices are moved radially outward slightly from a chosen point $0 \in$ Int $(\text{conv}(\mathcal{P}))$, see Figure 5.1.

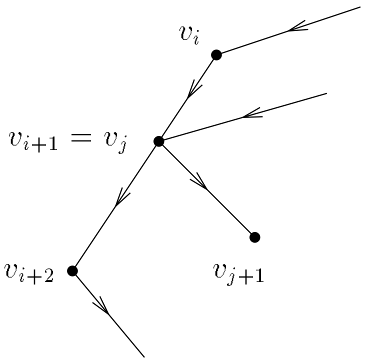

(i). Before

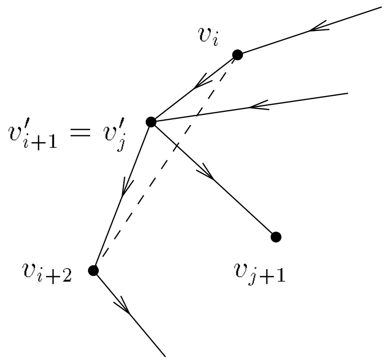

(ii). After

Figure 5.1: Eliminating collinear vertices

A sequence of properly chosen small deformations will preserve the CX-property, and destroy collinearity.

We next prove two lemmas which, when they apply, simplify the CX-polygon $\mathcal{P}$, while leaving the number of jumps unchanged. We define a *monotone boundary path* to be a path $[v_i, v_{i+1}, \ldots, v_{i+j}]$ where all edges are in $\partial\text{conv}(\mathcal{P})$ and no (undirected) edges are traversed twice, i.e., all vertices in the path are distinct, except possibly the end vertices of $j \geq 3$. Such a path has an *orientation*, either clockwise or counterclockwise.

Lemma 5.2 *If $\mathcal{P} = \langle v_0, v_1, \ldots, v_{n-1}\rangle$ is a boundary CX-polygon which contains a monotone boundary path $[v_i, v_{i+1}, \ldots, v_j]$ that completely traverses $\partial\text{conv}(\mathcal{P})$, then*

$$\mathcal{P}' = \langle v_0, v_1, \ldots, v_{i-1}, v_i, v_{j+1}, \ldots, v_{n-1}\rangle$$

is also a boundary CX-polygon.

Proof. By hypothesis $v_j = v_i$ and the polygon $\mathcal{P}'' = \langle v_i, v_{i+1}, \ldots, v_{j-1}\rangle$ is parametrization-equivalent to $\partial\text{conv}(\mathcal{P})$. Since $\mathcal{P}$ is a CX-polygon,

$$\mathcal{M}(\mathcal{P}'') = \frac{2\pi}{L(\partial\text{conv}(\mathcal{P}))} = \mathcal{M}(\partial\text{conv}(\mathcal{P})) > \mathcal{M}(\mathcal{P}) \ .$$

Now $L(\mathcal{P}') = L(\mathcal{P}) - L(\mathcal{P}'')$, and we also have

$$K(\mathcal{P}') \leq K(\mathcal{P}) - 2\pi ,$$

by direct computation of external angles at v_i and v_j. Thus

$$\mathcal{M}(\mathcal{P}') = \frac{K(\mathcal{P}')}{L(\mathcal{P}')} \leq \frac{K(\mathcal{P}) - 2\pi}{L(\mathcal{P}) - L(\partial \mathrm{conv}(\mathcal{P}))} \leq \mathcal{M}(\mathcal{P}) ,$$

hence $\mathcal{P}'$ is a CX-polygon. □

Lemma 5.3 *Let $P = \langle v_0, \ldots, v_{n-1} \rangle$ be a boundary CX-polygon. Suppose that $\mathcal{P}$ contains a jump $[v_i, v_{i+1}]$, with vertices v_{i+2} and v_{i-1} in opposite open half-spaces determined by the line $\ell[v_i, v_{i+1}]$, followed by a monotone boundary path $[v_{i+1}, v_{i+2}, \ldots, v_j]$ having $v_j = v_i$. Then*

$$\mathcal{P}' = \langle v_0, \ldots, v_{i-1}; v_j, v_{j-1}, v_{j-2}, \ldots, v_{i+1}, v_i; v_{j+1}, \ldots, v_{n-1} \rangle$$

is a boundary CX-polygon, and $\mathcal{M}(\mathcal{P}') \leq \mathcal{M}(\mathcal{P})$.

Proof. Here $\mathcal{P}'$ is obtained from $\mathcal{P}$ by replacing $[v_i, v_{i+1}, \ldots, v_j]$ by following the reversed monotone boundary path $[v_j, v_{j-1}, v_{j-2}, \ldots, v_{i+1}]$ and then taking the reversed jump $[v_{i+1}, v_i]$. There are two possibilities, depending on the location of v_{i-1} and v_{j+1} with respect to the line $\ell[v_i, v_{i+1}]$, see Figure 5.2.

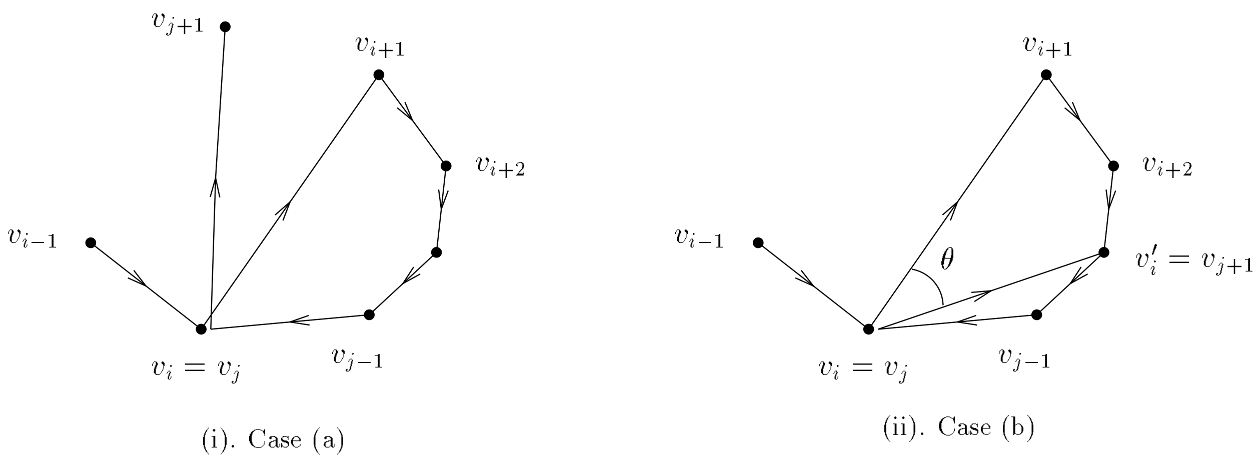

Figure 5.2: Configurations in Lemma 5.3.

Case (a) is where v_{i-1} and v_{j+1} are in the same open half-space determined by $\ell[v_i, v_{i+1}]$ or else v_{j+1} is on this line (which means $v_{j+1} = v_{i+1}$). A calculation[2] of the external angles at v_i gives

$$K(\mathcal{P}') = K(\mathcal{P}) \ .$$

Case (b) is where v_{j+1} and v_{i-1} are in opposite open half spaces determined by $\ell[v_i, v_{i+1}]$. We then have

$$K(\mathcal{P}') = K(\mathcal{P}) - 2\theta < K(\mathcal{P}) \ ,$$

where $\theta =$ angle (v_{i+1}, v_i, v_{j+1}), see Figure 5.2(ii). (In case (b) v_{j+1} necessarily coincides with some vertex in $v_{i+2}, \ldots, v_{j-1}$.)

In either case we have

$$\mathcal{M}(\mathcal{P}') = \frac{K(\mathcal{P}')}{L(\mathcal{P}')} \leq \mathcal{M}(\mathcal{P}) \ ,$$

so $\mathcal{M}(\mathcal{P}')$ is a CX-polygon. □

Proof of Theorem 5.1. It suffices to show that if there exists a boundary CX-polygon $\mathcal{P}$ having $m \geq 1$ jumps, then there exists a boundary CX-polygon $\mathcal{P}'$ having less jumps.

We give five situations below under which a boundary CX-polygon $\mathcal{P}'$ with fewer jumps can be constructed from $\mathcal{P}$. Then we prove that given any boundary CX-polygon, we can construct another boundary CX-polygon having the same number of jumps, to which one of the reductions *J1–J5* below applies.

Reduction J1. $\mathcal{P}$ contains a jump $[v_i, v_{i+1}]$ such that v_{i-1} and v_{i+2} are in the same closed half-space of $\ell[v_i, v_{i+1}]$.

In this case, since $[v_i, v_{i+1}]$ is a jump there are vertices of $\mathcal{P}$ in the open half-space of $\ell[v_i, v_{i+1}]$ not containing v_{i-1} and v_{i+2}. By ordering them properly we get a convex path $u_1 = v_i,\ u_2, \ldots, u_j = v_{i+1}$ see Figure 5.3. Take the boundary polygon

$$\mathcal{P}' = \langle v_0, \ldots, v_{i-1};\ u_1, \ldots, u_j; v_{i+2}, \ldots, v_n \rangle \ .$$

Then $K(\mathcal{P}') = K(\mathcal{P})$ but clearly $L(\mathcal{P}') > L(\mathcal{P})$. Hence $\mathcal{M}(\mathcal{P}') < \mathcal{M}(\mathcal{P})$, and $\mathcal{P}'$ is a boundary CX-polygon with one less jump.

Reduction J2. $\mathcal{P}$ contains two consecutive jumps $[v_i, v_{i+1}]$ and $[v_{i+1}, v_{i+2}]$.

[2] This holds even if $[v_{i-1}, v_i]$ is a jump.

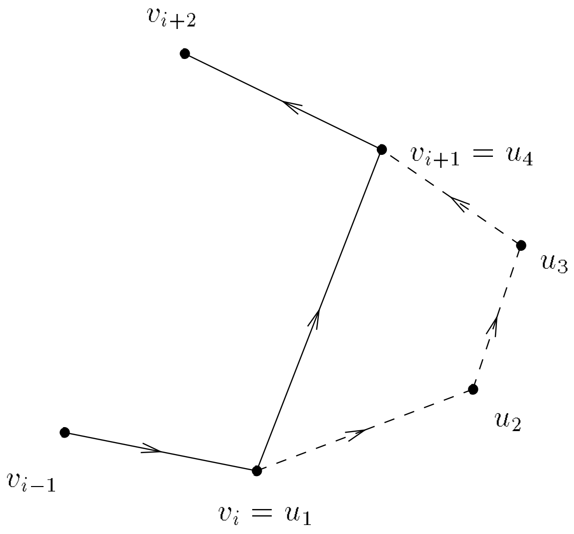

Figure 5.3: Reduction J1

First, v_{i-1} and v_{i+2} must be an opposite open halfspaces determined by $\ell[v_i, v_{i+1}]$, or else reduction J1 applies. Similarly v_i and v_{i+3} are in opposite open half-spaces determined by $\ell[v_{i+1}, v_{i+2}]$, or else reduction J1 applies. We now have the configuration pictured in Figure 5.4.

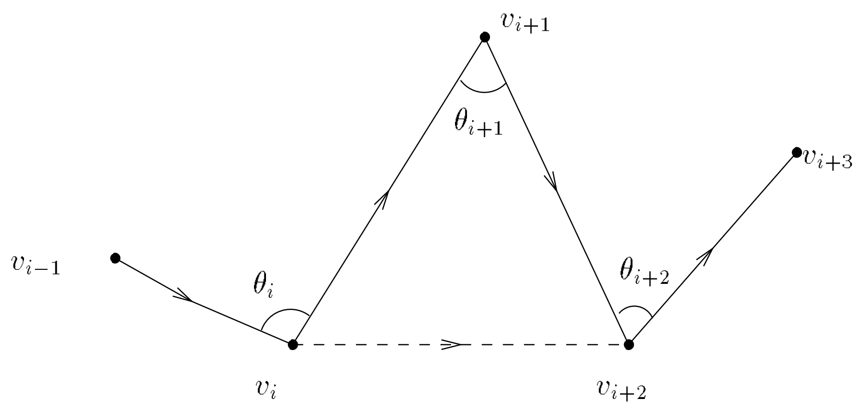

Figure 5.4: Reduction J2

The boundary polygon

$$\mathcal{P}' = \langle v_0, \ldots, v_i, v_{i+2}, v_{i+3}, \ldots, v_{n-1} \rangle$$

has fewer jumps. Convexity forces v_{i-1} and v_{i+3} to be in the same closed half-space determined by the line $\ell[v_i, v_{i+2}]$, so the hypotheses of Lemma 4.3 hold for $\mathcal{P}$ with $\mathcal{Q} = \langle v_i, v_{i+1}, v_{i+2} \rangle$, hence $\mathcal{P}'$ is a CX-polygon.

Reduction J3. $\mathcal{P}$ contains a jump $[v_i, v_{i+1}]$, the path $[v_{i+1}, v_{i+2}, \ldots, v_{j+1}]$ is a monotone boundary path followed by a reversal $v_{j+2} = v_j$, and in addition $v_i \notin \{v_{i+1}, \ldots, v_j\}$.

We may assume that v_{i+2} and v_{i-1} are on opposite sides of the line $\ell[v_i, v_{i+1}]$, otherwise reduction J1 applies. This situation is pictured in Figure 5.5.

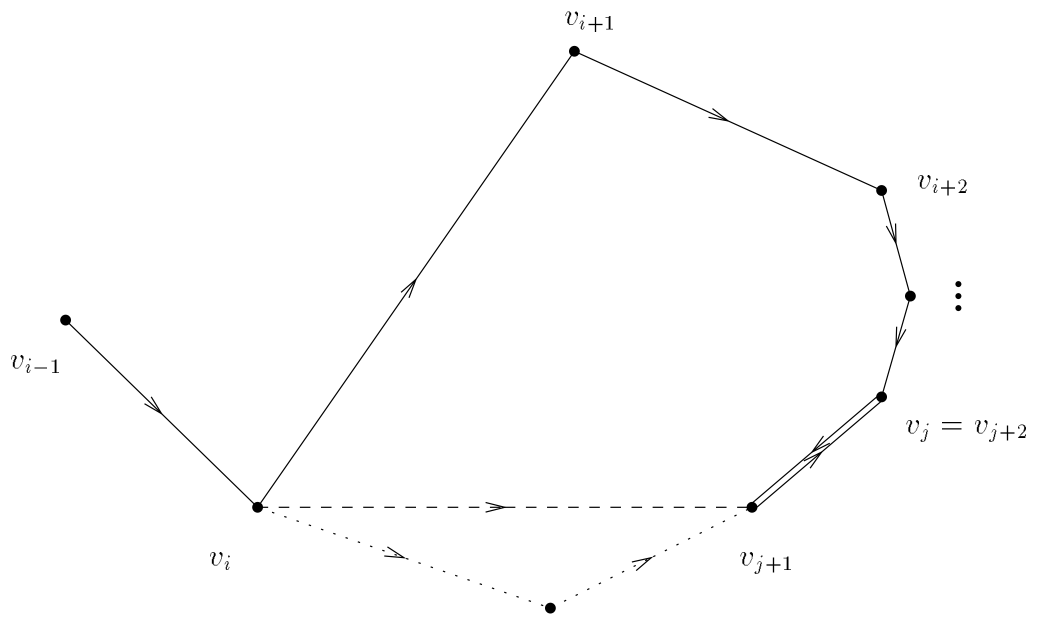

Figure 5.5: Reduction J3 (case $v_i \neq v_{j+1}$).

If $v_i = v_{j+1}$, then consider the boundary polygon

$$\mathcal{P}' = \langle v_0, \ldots, v_i, v_{j+2}, v_{j+3}, \ldots, v_{n-1} \rangle \ ,$$

which has one less jump than $\mathcal{P}$. Now the hypotheses of Lemma 4.4 apply to $\mathcal{P}$ with $\mathcal{Q} = [v_i, v_{i+1}, \ldots, v_{j+1}]$, hence $\mathcal{P}'$ is a CX-polygon.

If $v_i \neq v_{j+1}$, then consider instead the boundary polygon

$$\mathcal{P}' = \langle v_0, \ldots, v_i, v_{j+1}, v_{j+2}, \ldots, v_{n-1} \rangle \ .$$

We apply Lemma 4.3, taking $\mathcal{Q} = \langle v_i, v_{i+1}, \ldots, v_{j+1} \rangle$, to conclude that $\mathcal{P}'$ is a CX-polygon. However, it may be that $[v_i, v_{j+1}]$ is a jump so that the number of jumps has not decreased. But if so, then reduction J1 immediately applies to this jump, so it can be removed.

Reduction J4. $\mathcal{P}$ contains the jump $[v_i, v_{i+1}]$, followed by a monotone boundary path $[v_{i+2}, \ldots v_j]$, then $[v_j, v_{j+1}]$ is a jump which either does not touch $[v_i, v_{i+1}]$, or else $v_{j+1} = v_i$. Furthermore $v_i \notin \{v_{i+1}, \ldots, v_j\}$.

Here v_{i-1} and v_{i+2} are in opposite open half-spaces determined by $\ell(v_i, v_{i+1})$, otherwise reduction J1 or J2 applies. The resulting situation is pictured in Figure 5.6.

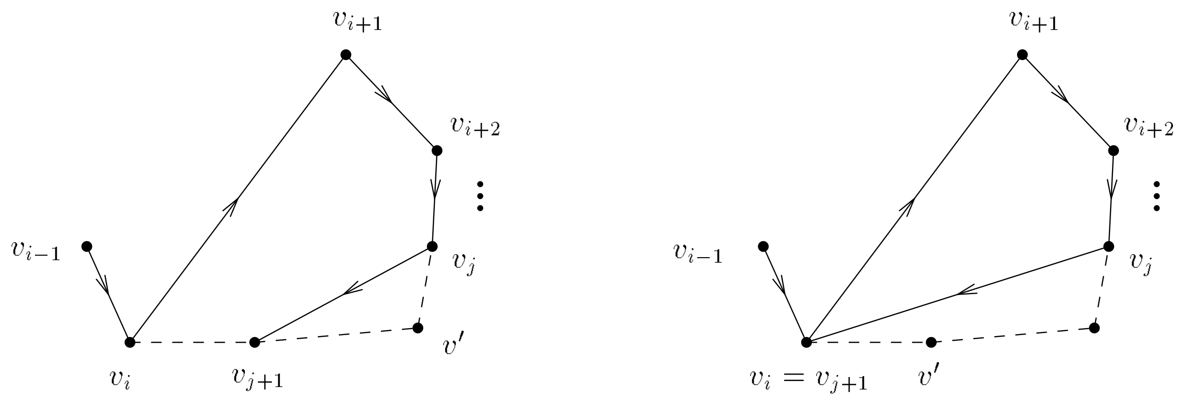

(i). General Case ($v_i \neq v_{j+1}$)

(ii). Special Case ($v_i = v_{j+1}$)

Figure 5.6: Reduction J4

Consider the "general case" that $v_{j+1} \neq v_i$, pictured in Figure 5.6(i). If v_{j+2} is in the closed half-space containing v_i with boundary line $\ell[v_j, v_{j+1}]$, then the jump $[v_j, v_{j+1}]$ can be removed by reduction J1. (This includes the case $v_{j+2} = v_i$.) So suppose v_{j+2} is in the opposite open half-space from v_i determined by the line $\ell[v_j, v_{j+1}]$. Now the hypotheses of Lemma 4.3 are fulfilled for $\mathcal{P}$ with $\mathcal{Q} = \langle v_i, v_{i+1}, \ldots, v_{j+1} \rangle$, so we conclude that the boundary polygon

$$\mathcal{P}' = \langle v_0, \ldots, v_i, v_{j+1}, \ldots, v_n \rangle$$

is a CX-polygon. Since $\mathcal{P}'$ removes two jumps and possibly adds one jump with respect to $\mathcal{P}$, it has fewer jumps.

There remains the "special case" where $v_{j+1} = v_i$, pictured in Figure 5.6(ii). As in the case above, v_{j+2} lies in the open half-space separated from v_{i+1} by $\ell[v_j, v_{j+1}]$. We consider the boundary polygon

$$\mathcal{P}' = \langle v_0, \ldots, v_i, v_{j+2}, \ldots, v_n \rangle$$

which has two fewer jumps than $\mathcal{P}$. We conclude that $\mathcal{P}'$ is a CX-polygon by an application of Lemma 4.4 to $\mathcal{P}$, with $\mathcal{Q} = [v_i, v_{i+1}, \ldots, v_j, v_{j+1}]$.

Reduction J5. $\mathcal{P}$ contains a monotone boundary path $[v_h, v_{h+1}, \ldots, v_i]$, followed by the jump $[v_i, v_{i+1}]$, followed by a monotone boundary path $[v_{i+1}, \ldots, v_j]$ followed by a jump $[v_j, v_{j+1}]$ which either crosses $[v_i, v_{i+1}]$, i.e., $(v_i, v_{i+1}) \cap (v_j, v_{j+1}) \neq \varnothing$, or else $v_{j+1} = v_{i+1}$. This is then followed by a monotone boundary path $[v_{j+1}, v_{j+2}, \ldots, v_k]$ such that $v_k = v_h$. Furthermore $v_i \notin \{v_{i+1}, \ldots, v_j\}$.

First, reductions J1 or J2 can be used to remove one or the other of the two jumps unless $\mathcal{Q}_1 = \langle v_{i+1}, v_{i+2}, \ldots, v_j \rangle$ and $\mathcal{Q}_2 = \langle v_{j+1}, \ldots, v_k = v_h, v_{h+1}, \ldots, v_i \rangle$ are both convex polygons whose convex hulls are disjoint, except in the "special case" $v_{j+1} = v_{i+1}$, in which case they intersect in a point. The situation is pictured in Figure 5.7(i) and (ii). The path pictured in the "general case" is exactly the generalized crossing quadrilateral in Lemma 3.2.

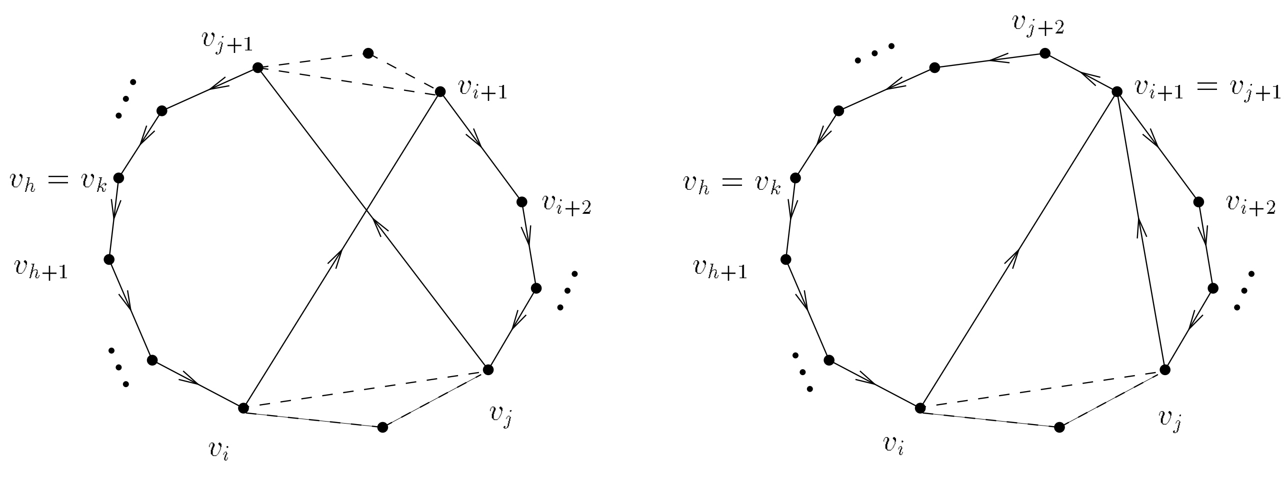

(i). General case ($v_{i+1} \neq v_{j+1}$) (ii). Special case ($v_{i+1} = v_{j+1}$)

Figure 5.7: Reduction J5

The polygon $\mathcal{P} = \langle v_0, \dots, v_{n-1} \rangle$ is a concatenation of the polygonal arcs

$$\mathcal{P}_1 = [v_h, v_{h+1}, \dots, v_i, v_{i+1}, \dots, v_j, v_{j+1}, \dots, v_k]$$

and

$$\mathcal{P}_2 = [v_k, v_{k+1}, \dots, v_{n-1}, v_0, v_1, \dots v_h] \; .$$

We associate to these the boundary polygons

$$\begin{aligned} \mathcal{P}_1' &= \langle v_h, v_{h+1}, \dots, v_{k-1} \rangle \; , \\ \mathcal{P}_2' &= \langle v_k, v_{k+1}, \dots, v_h, v_0, \dots, v_{h-1} \rangle \; . \end{aligned}$$

We obviously have

$$L(\mathcal{P}_1') + L(\mathcal{P}_2') = L(\mathcal{P}_1) + L(\mathcal{P}_2) = L(\mathcal{P}) \; .$$

Using the fact that $[v_h, v_{h+1}]$ and $[v_{k-1}, v_k]$ are boundary edges, a calculation of exterior angles at $v_k = v_h$ yields

$$K(\mathcal{P}_1') + K(\mathcal{P}_2') \le K(\mathcal{P}) \; .$$

Combining this with the last equality yields

$$\min(\mathcal{M}(\mathcal{P}_1'), \mathcal{M}(P_2')) \le \mathcal{M}(\mathcal{P}) \; .$$

If $\mathcal{M}(\mathcal{P}_2') \le \mathcal{M}(\mathcal{P})$ then $\mathcal{P}_2'$ is a CX-polygon, and it has two fewer jumps than $\mathcal{P}$. If $\mathcal{M}(\mathcal{P}_1') \le \mathcal{M}(\mathcal{P})$, then $\mathcal{P}_1'$ is a CX-polygon, and it also has fewer jumps than $\mathcal{P}$, unless $\mathcal{P}_2'$ has no jumps.

There remains a final case in which $\mathcal{P}_1'$ is a CX-polygon with two jumps, and $\mathcal{P}_2'$ has no jumps. We consider two subcases according as $v_{j+1} \ne v_{i+1}$ or not. In the "general case" where $v_{j+1} \ne v_{i+1}$ we can immediately apply Lemma 3.2 to conclude that $\mathcal{M}(P_1'') < \mathcal{M}(P_1')$, where

$$\mathcal{P}_1'' = \langle v_h, v_{h+1}, \dots, v_i; v_j, v_{j-1}, \dots, v_{i+1}; v_{j+1}, v_{j+2}, \dots, v_{k-1} \rangle \; .$$

Thus $\mathcal{P}_1''$ is a boundary CX-polygon, but it may still have two jumps, namely $[v_i, v_j]$ and $[v_{i+1}, v_{j+1}]$. However both these jumps occur in an arrangement where they can be eliminated by reduction J1, completing the "general case.". Finally, in the "special case" where $v_{j+1} = v_{i+1}$, we use Lemma 3.2 with a limiting argument (using a distinct v_{j+1} and letting $v_{j+1} \to v_{i+1}$) to conclude that $\mathcal{M}(\mathcal{P}_1'') \le \mathcal{M}(\mathcal{P}_1')$, where

$$\mathcal{P}_1'' = \langle v_h, v_{h+1}, \dots, v_i; v_j, v_{j-1}, \dots, v_{i+1}; v_{j+2}, \dots, v_{k-1} \rangle \; .$$

Thus $\mathcal{P}_1''$ is a boundary CX-polygon with at most two jumps, and reduction J1 can be applied to $\mathcal{P}_1''$ if necessary to reduce the number of jumps to zero.

Induction Step. We may assume that $\mathcal{P} = \langle v_0, v_1, \ldots, v_{n-1} \rangle$ is a boundary CX-polygon with no three vertices collinear. We produce a boundary CX-polygon on a subset of the vertices of $\mathcal{P}$ which has fewer jumps.

Suppose that the location of the m jumps of $\mathcal{P}$ are $[v_{i_1}, v_{i_1+1}], [v_{i_2}, v_{i_2+1}], \ldots, [v_{i_m}, v_{i_m+1}]$, where $0 \leq i_1 < \ldots < i_m \leq n-1$. We proceed by a sub-induction on the number of edges n in $\mathcal{P}$, and show either that n can be decreased while holding the number of jumps constant, or else a jump can be removed. In particular, this process must eventually halt with a jump being removed, thus completing the induction step.

For the sub-induction, we consider cases.

(1). We show that each boundary arc $\mathcal{Q}_k := [v_{i_k+1}, v_{i_k+2}, \ldots, v_{i_{k+1}}]$ can be taken to be a monotone boundary path, having at least one line segment, or else a jump can be removed. (This includes the wrap-around case $k = m$, where we define $i_{m+1} = i_1$.)

To establish this, we can assume that there are no two consecutive jumps in $\mathcal{P}$ or else reduction J2 can be applied. Next, if some boundary arc $\mathcal{Q}_k$ contains a complete monotone traversal of the boundary $\partial conv(\mathcal{P})$, then we can apply Lemma 5.2 to remove it, thus reducing n and completing the sub-induction step. If not, and if $\mathcal{P}$ contains a non-monotone boundary arc $\mathcal{Q}_k = [v_{i_k+1}, \ldots, v_{i_{k+1}}]$, then $\mathcal{Q}_k$ must contain a reversal. The first line segment $[v_{i_k+1}, v_{i_k+2}]$ in $\mathcal{Q}_k$ must have the opposite boundary orientation to $[v_{i_k-1}, v_{i_k}]$ or else reduction J1 can be applied. If the boundary arc $\mathcal{Q}_k$ reverses direction at some vertex v_j, which is at or before the vertex v_{i_k}, then reduction J3 applies. Otherwise $\mathcal{Q}_k$ is a monotone boundary path all the way to a vertex $v_j = v_{i_k}$, and there is no reversal at v_j, i.e. $v_{j+1} = v_{i_k-1}$. In that case, we may apply Lemma 5.3 to obtain the boundary CX-polygon $\mathcal{P}'$ which is obtained from $\mathcal{P}$ by replacing the jump $[v_{i_k}, v_{i_k+1}]$ and the boundary arc $\mathcal{Q}_k$ with the reversed arc $\mathcal{Q}'' := [v_j, v_{j-1}, \ldots, v_{i_k+1}]$ followed by the reversed jump $[v_{i_k+1}, v_{i_k}]$, then followed by the (non-reversed) boundary arc $Q_k' := [v_j, v_{j+1}, \ldots, v_{i_k+1}]$. Now $\mathcal{P}'$ has the same number of jumps as $\mathcal{P}$, and its boundary arc $\mathcal{Q}_k'$ contains a reversal that it inherited from $\mathcal{Q}_k$. This reversal must occur before vertex v_{i_k+1} is reached, otherwise $\mathcal{Q}_k$ would have contained a complete monotone transversal of the boundary $\partial conv(\mathcal{P})$. It follows that reduction J3 applies to $\mathcal{P}'$, to give a boundary CX-polygon with one less jump.

(2). We may suppose that any two consecutive monotone boundary paths $\mathcal{Q}_k$ and $\mathcal{Q}_{k+1}$ are oppositely oriented on the boundary ∂R, otherwise the jump $[v_{i_k}, v_{i_k+1}]$ could be removed using reduction J1. It follows that there are an even number of jumps.

(3). We next reduce to the case that every (monotone) boundary path $\mathcal{Q}_k = [v_{i_k+1}, \ldots, v_{i_{k+1}}]$ has

$$v_{i_k} \notin \{v_{i_k+1}, \ldots, v_{i_{k+1}}\} \ . \tag{5.1}$$

For if this condition is violated for $\mathcal{Q}_k$, then we may apply Lemma 5.3, to get a CX-polygon P' in which the jump $[v_{i_k}, v_{i_k+1}]$ is shifted and replaced with a reversed jump $[v_{i_k+1}, v_{i_k}]$. If Lemma 5.3 applies once more to the jump $[v_{i_k+1}, v_{i_k}]$ in P', then, as in step (1), P would contain a complete monotone circuit of $\partial\mathrm{conv}(\mathcal{P})$ and we could delete it using Lemma 5.2, thus decreasing n and completing the sub-induction step in this case. Now assume that Lemma 5.3 applies only once at the k-th jump, so that it eliminates the violation of (5.1) at the k-th path $\mathcal{Q}_k$. In applying Lemma 5.3 we note that only $\mathcal{Q}_{k-1}$ and $\mathcal{Q}_k$ are changed, hence it could introduce a new violation of (5.1) only at $\mathcal{Q}_{k-1}$. The monotone boundary path $\mathcal{Q}_{k-1}$ is extended by concatenating to it $[v_j, v_{j-1}, \ldots, v_{i_k+1}]$, where $v_j = v_{i_k}$ and $j \in \{i_k+1, i_k+2, \ldots, i_{k+1}\}$. Thus, if (5.1) applies to the $(k-1)$-st path in $\mathcal{P}'$, but not to the $(k-1)$-st path in $\mathcal{P}$, then necessarily $v_{i_{k-1}} \in \mathcal{Q}_k$, and reduction J5 applies to the pair of jumps $[v_{i_{k-1}}, v_{i_{k-1}+1}]$ and $[v_{i_k}, v_{i_k+1}]$ in $\mathcal{P}$, and removes a jump. Thus there remains the case where this operation makes (5.1) hold for $\mathcal{Q}_k$, and does not change whether (5.1) holds or doesn't hold at any other $\mathcal{Q}_\ell$. Repeating this procedure, at most m applications of Lemma 5.3 guarantee that (5.1) holds at all k. (The role of (5.1) is to allow reductions J4 and J5 to be applied.)

(4). We now consider two consecutive jumps $[v_{i_k}, v_{i_k+1}]$ and $[v_{i_{k+1}}, v_{i_{k+1}+1}]$. If they do not cross then reduction J4 applies to these jumps, since (5.1) holds.

(5). The final case remaining is where every two consecutive jumps $[v_{i_k}, v_{i_k+1}]$ and $[v_{i_{k+1}}, v_{i_{k+1}}]$ cross. Call their intersection point x_k. We show that reduction J5 must apply to some pair of consecutive jumps. The critical configuration is depicted in Figure 5.8(ii). The lines $\ell_k := \ell[v_{i_k}, v_{i_k+1}]$ and $\ell_{k+1} := \ell[v_{i_{k+1}}, v_{i_{k+1}+1}]$ partition $\mathbb{R}^2$ into four cones, each pointed at x_k. Of these we let C_k denote the closed cone $C^+[x_k; v_{i_k+1} - x_k,\ v_{i_{k+1}+1} - x_k]$, see Figure 5.8(ii). We will prove that, under the assumption that reduction J5 does not apply to the jumps ℓ_k at

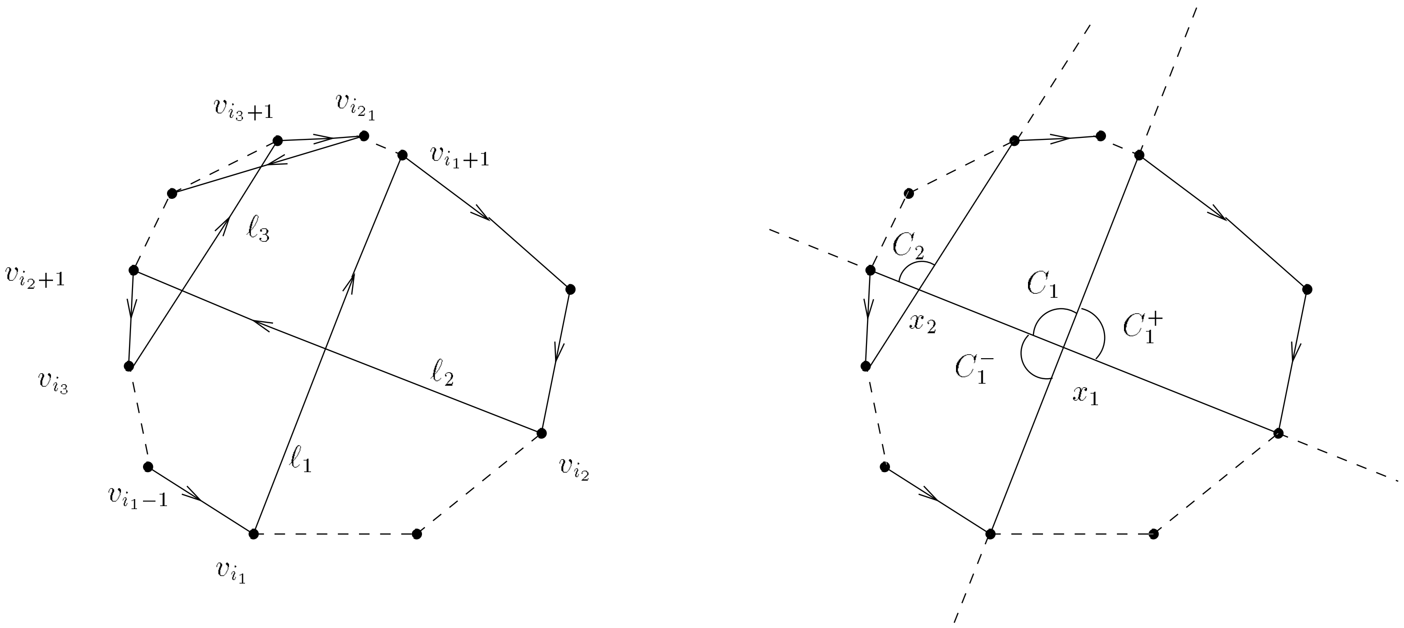

Figure 5.8: Sub-induction step

ℓ_{k+1}, that

$$C_{k+1} \cap \operatorname{conv}(\mathcal{P}) \subsetneqq C_k \cap \operatorname{conv}(\mathcal{P}) \ . \tag{5.2}$$

In particular, if reduction J5 never applies, then we cycle through all jumps and come back to C_1, to obtain

$$C_1 \cap \operatorname{conv}(P) \subsetneqq C_1 \cap \operatorname{conv}(P) \ ,$$

a contradiction that will complete the sub-induction step.

It remains to prove (5.2). For notational convenience we suppose that $k = 1$. Set $C_1^+ := C^+[x_1; x_1 - v_{i_1}, v_{i_2} - x_1]$. It is a cone pointed at x_1 with boundary in $\ell_1 \cup \ell_2$, which contains the monotone path $[v_{i_1+1}, \ldots, v_{i_2}]$. Let $C_1^- := C^+[x_1; v_{i_1} - x_1, x_1 - v_{i_2}]$ be the cone obtained from C_1^+ by reflection about x_1, see Figure 5.8(ii). Then the monotone paths $[v_{i_2+1}, \ldots, v_{i_3}]$ and $[v_{i_m+1}, \ldots, v_{i_1}]$ both lie in C_1^- and are disjoint, for if they overlap then reduction J5 applies to the jumps at v_{i_m} and v_{i_1}. We next show that v_{i_3+1} lies in the interior of C_1. Certainly v_{i_3+1} lies in $C_1 \cup C_1^+$ because $[v_{i_3}, v_{i_3+1}]$ crosses $[v_{i_2}, v_{i_2+1}]$ in the interior of $\operatorname{conv}(\mathcal{P})$, say at the point x_2. Also $v_{i_3+1} \notin C_1^+$ or else $v_{i_3+1} \in \{v_{i_1+1}, \ldots, v_{i_2}\}$, in which case reduction J5 applies to the jumps at v_{i_2} and v_{i_3}. Furthermore $v_{i_3+1} \neq v_{i_2+1}$, so v_{i_3+1} lies strictly in the interior of C_1. Now x_2 lies in C_1, because C_1^- is adjacent to the cone C_1 but not to C_1^+. Hence, the whole edge $[x_2, v_{i_3+1}]$ lies in C_1. Thus, the cone $C_2 = C^+[x_2; v_{i_2+1} - x_2, v_{i_3+1} - x_2]$ has

$$C_2 \cap \mathrm{conv}(P) \subsetneqq C_1 \cap \mathrm{conv}(P) \ ,$$

where strict inclusion holds because v_{i_3+1} is on a boundary edge of C_2 but is strictly interior to C_1. Thus (5.2) holds. $\square$

6 Average Curvature Theorem

Proof of Theorem 1.1. We argue by contradiction. The combination of Lemma 2.2, Theorem 4.1 and Theorem 5.1 shows that if there is a counterexample, then there exists a boundary CX-polygon $\mathcal{P} = \langle v_0, v_1, \ldots, v_{n-1} \rangle$ such that all edges of $\mathcal{P}$ lie in the set $\partial\mathrm{conv}(\mathcal{P})$. The polygon $\mathcal{P}$ can be partitioned into a set of monotone boundary paths, with a reversal marking the ends of each such path. A *reversal* is a set of consecutive boundary edges $[v_i, v_{i+1}]$ and $[v_{i+1}, v_{i+2}]$ with $v_{i+2} = v_i$. If a monotone boundary path contains a subpath that completely encircles $\partial\mathrm{conv}(\mathcal{P})$, then we can snip that piece out using Lemma 5.2, and still have a CX-polygon. Thus we may suppose all such monotone boundary paths have at most $n-1$ segments. If $\mathcal{P}$ had no reversals, then $\mathcal{P}$ is parametrization-equivalent to $k * \partial(\mathrm{conv}\mathcal{P})$ for some nonzero integer k, hence $\mathcal{M}(\mathcal{P}) = \frac{2\pi}{L(\partial\mathrm{conv}(\mathcal{P}))}$. This contradicts $\mathcal{P}$ being a CX-polygon.

Now suppose that $\mathcal{P}$ contains $m \geq 1$ reversals. Then $m \geq 2$, since $\mathcal{P}$ is closed. We prove that there exists a boundary CX-polygon with no jumps and fewer than m reversals. By downwards induction there exists one with no reversals, which is impossible.

For the induction step, suppose first that $\mathcal{P}$ contains two adjacent reversals, i.e. a subpath $[v_i, v_{i+1}, v_{i+2}, v_{i+3}]$ with $v_{i+2} = v_i$ and $v_{i+3} = v_{i+1}$. Then the new polygon

$$\mathcal{P}' = [v_0, \ldots, v_i, v_{i+1}, v_{i+4}, \ldots, v_{n-1}]$$

is a boundary polygon with no jumps and it has two fewer reversals. It is a CX-polygon since

$$\mathcal{M}(\mathcal{P}') = \frac{K(\mathcal{P}')}{L(\mathcal{P}')} = \frac{K(\mathcal{P}) - 2\pi}{L(\mathcal{P}) - 2||v_{i+1} - v_i||} \leq \mathcal{M}(\mathcal{P}) \ ,$$

using

$$\frac{2\pi}{2||v_{i+1}-v_i||} \geq \frac{2\pi}{L(\partial \mathrm{conv}(\mathcal{P}))} > \frac{K(\mathcal{P})}{L(\mathcal{P})} \,.$$

It remains to consider the case where $\mathcal{P}$ contains two consecutive reversals that are not directly adjacent. That is, $\mathcal{P}$ contains a path $[v_i, v_{i+1}, \ldots, v_{j+1}, v_{j+2}]$ in which $v_{i+2} = v_i$ and $v_{j+2} = v_j$, where $\mathcal{Q} = [v_{i+1}, v_{i+2}, \ldots, v_{j+1}]$ is a monotone boundary path of length $\leq n-1$. Now Lemma 4.3 applies to show that the polygon

$$\mathcal{P}' = \langle v_0, \ldots, v_{i+1}, v_{j+1}, \ldots v_{n-1} \rangle$$

has

$$\mathcal{M}(\mathcal{P}') \leq \mathcal{M}(\mathcal{P}) \,,$$

and is a boundary CX-polygon. However $[v_{i+1}, v_{j+1}]$ may now be a jump. To remove the jump, let $\mathcal{Q}^c = [v_{i+1}, u_1, \ldots, u_k, v_{j+1}]$ be the monotone path from v_{i+1} to v_{j+1} in $\partial\mathrm{conv}(\mathcal{P})$ that lies in the complement of $[v_{i+2}, v_{i+3}, \ldots, v_j]$. Then consider

$$\mathcal{P}'' = \langle v_0, \ldots, v_i, v_{i+1}, u_1, \ldots, u_k, v_{j+1}, \ldots, v_{n-1} \rangle \,,$$

which is a boundary polygon with no jumps and which has two fewer reversals than $\mathcal{P}$, see Figure 6.1.

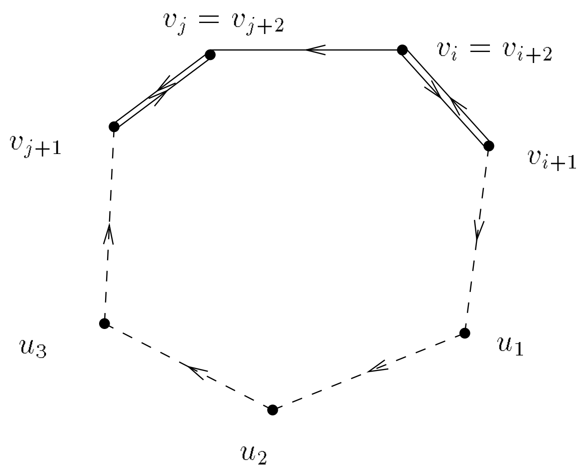

Figure 6.1: Complementing paths. (In this figure $Q^c = [v_{v+1}, u_1, u_2, u_3, v_{j+1}]$.)

We have $K(\mathcal{P}'') = K(\mathcal{P}')$, using the fact that the closed polygon $\langle v_{i+1}, u_1, \ldots, u_k, v_{j+1}\rangle$ is convex, and clearly $L(\mathcal{P}'') \geq L(\mathcal{P}')$, hence

$$\mathcal{M}(\mathcal{P}'') \leq \mathcal{M}(\mathcal{P}') \ .$$

Thus $\mathcal{M}(\mathcal{P}'') \leq \mathcal{M}(\mathcal{P})$, so $\mathcal{P}''$ is a CX-polygon. This completes the induction step, and the proof. $\square$

References

[1] T. Banchoff, Critical Points and Curvature for Embedded Polyhedra, J. Diff. Geom. **1** (1967), 257–268.

[2] T. Banchoff, Critical Points and Curvature for Embedded Polyhedral Surfaces, Amer. Math. Monthly **77** (1970), 475–485.

[3] Yu D. Burago and V. A. Zalgaller, *Geometric Inequalities*, Springer-Verlag: Boston, 1988.

[4] J. Cheeger, W. Müller, and R. Schrader, On the Curvature of Piecewise Flat Spaces, Comm. Math. Phys. **92** (1984), 405–454.

[5] J. Cheeger, W. Müller, and R. Schrader, Kinematic and Tube Formulas for Piecewise Linear Spaces, Indiana U. Math. J. **35** (1986), 737–754.

[6] S. S. Chern, Curves and Surfaces in Euclidean Space, in: *Studies in Global Geometry and Analysis*, (C. W. Curtis, Ed.), MAA, 1967, pp. 16–56.

[7] I. Fáry, Sur certaines inégalitiés géométriques, Acta. Sci. Math. (Szeged) **12** (1950), 117–124.

[8] F. J. Flaherty, Curvature Measures for Piecewise Linear Manifolds, Bull. Amer. Math. Soc. **79** (1973), 100–102.

[9] G. Galperin and A. Topygo, *Moscow Mathematical Olympiads*, Education: Moscow 1986. (Russian) (Problem #33).

[10] J. Milnor, On the Total Curvature of Knots, Annals of Math. **52** (1950), 248–257.

[11] T. J. Richardson, Total Curvature and Intersection Tomography, Advances in Mathematics, to appear.

[12] L. A. Santaló, *Integral Geometry and Geometric Probability*, Addison-Wesley: Reading, Massachusetts, 1976.

[13] R. Schneider, *Convex Bodies: The Brunn-Minkowski Theory*, Cambridge U. Press: Cambridge, 1993.

[14] J. Steiner, Über parallel flächen, Jber. preuss. Akad. Wiss. (1840), 114–118. (See: *Gesammelte Werke*, Vol. II, New York: Chelsea 1971, pp. 171–177.)

[15] H. Steinhaus, Length, shape, and area, *Colloq. Math.*, **3**, (1954) 1-13.